A COMPARATIVE STUDY OF SNOWMELT-DRIVEN WATER BUDGETS IN ADJACENT ALPINE BASINS, NIWOT RIDGE, COLORADO FRONT RANGE

By

Ian M. Nesbitt

Professor David P. Dethier
Advisor

A thesis
Submitted in partial fulfillment of the requirements for the
Degree of Bachelor of Arts
With Honors in Geosciences

Williams College
Williamstown, Massachusetts

Friday, May 17, 2013

ACKNOWLEDGEMENTS

Dedicated to my loving parents. Mom and Dad, I'm not sure you knew what you were getting into when you started called me "Hydro-Ian" as a kid. "Hydro-Ian" has now taken me from little streams on Pine Cobble Road to little streams in the Colorado Front Range. I'm excited to find out where it will take me next. Without your tireless belief in me and your investment in my education, none of the things I've achieved in the last four years would be possible.

I love you. Thank you.

CONTENTS

LIST OF FIGURES

LIST OF TABLES

LIST OF EQUATIONS

LIST OF APPENDICES

ABSTRACT

The Critical Zone, which extends from the top of the weathered bedrock to the tops of the tallest vegetation in alpine and subalpine headwater areas delivers fresh water to urban corridors near mountainous areas of North America. Snowmelt runoff from alpine basins typically accounts for over 80% of annual flow, but water budgets are not well quantified nor well understood in detail. Redistribution of snow by wind, the difficulty of estimating water losses from sublimation and evapotranspiration, and groundwater gains and losses from outside the basin make streamflow and water budget measurements challenging. I investigated two adjacent 0.25 km^2 catchments, Martinelli and Saddle streams, both at ~3500 m, on Niwot Ridge in the Colorado Front Range. Mean annual runoff is ~230 mm (25% of mean annual precipitation) at Saddle basin and ~310 mm (30% of mean annual precipitation) at Martinelli basin, based on 12 and 28 years of gaging records, respectively.

Saddle stream is not fed by a late-lying snowpack, but records indicate that ablation-season discharge is still closely related to snowmelt in the basin. Martinelli basin shelters a ~6 m thick snowpatch in 8 ha of the basin, even in a low snow year. During much of the ablation season, snowpack mass density (ρ) is 0.5 g cm^{-3} and ablation rates are ~100 mm day^{-1}. Since vegetation is shallow-rooted or nonexistent in Martinelli, evapotranspiration (ET) is probably not a major factor. Saddle basin is more heavily vegetated, but only the lower reaches are wooded; ET is likely < 260 mm annually. Specific runoff measured at the gage during 2012 was ~270 mm at Martinelli and ~35 mm at the Saddle gage. By monitoring snowpack area changes and longitudinal discharge, we were able to demonstrate that at least 30% of annual precipitation in Martinelli basin and 10% in Saddle basin bypasses the gage as subsurface flow. Short-term yield calculations indicate that approximately 2.5% of precipitation discharges from the basin as measurable surface water within a five-day period; the rest recharges

groundwater or becomes immeasurable subsurface flow. For comparison, a nearby 2.3 km^2 glaciated basin, Green Lake 4, discharges 50% of the water that falls on it within the same five-day period. Measured water yields from small, unglaciated alpine catchments thus should be viewed with caution.

INTRODUCTION

Fresh water in the western continental U.S. is a scarce resource that is becoming more difficult to obtain (Miller and Piechota, 2011). The discharge of mountain streams is closely monitored in many areas to ensure the proper amount is allocated from runoff and storage to supply the needs of downstream agriculture and municipalities. Because seasonal snowmelt generates a large percentage of fresh drinking water in the western USA, the processes governing its distribution and melt rate must be understood to better predict the amount of runoff and hence water storage and use restrictions. Monitoring of surface discharge emphasizes large streams or main tributaries, because these are the most economically significant and easiest to measure. Small catchments are less closely monitored, but a clear understanding of catchment-scale processes is vital to predicting the timing and flow in larger basins downstream.

Small (<10 km^2) alpine catchments cover significant area in the headwaters of Colorado river basins. These catchments vary widely in both open-channel and subsurface flow, depending on factors including precipitation characteristics, snowpack distribution, and surficial materials, complicating efforts to construct comprehensive regional runoff models. Climate change poses additional challenges, both for obtaining water and for predicting temporal shifts in surface and groundwater flow from alpine regions (Lapp et al, 2005; Laghari et al., 2012). Present groundwater contributions to alpine runoff exceed 50% in some basins (Liu et al., 2004; Clow et al., 2003). Understanding water storage and transmission characteristics of these basins is critical to predicting how alpine discharge will change over time as climate warms (Day, 2009).

The central concept of a water budget is that in a watertight basin, the input quantity of water equals the output plus evapotranspiration. If the inputs and outputs (measured and assumed) do not equal one another, some combination of the measurements or assumptions is incorrect (i.e. perhaps the basin is leaky). The focus of this project is using measured and estimated values to examine short- and long-term water budgets for two adjacent basins, Martinelli and Saddle, to attempt to observe and quantify a significant disparity between measured precipitation and discharge values.

Ground and surface water hydrology: interactions in the Critical Zone

Anderson and Anderson (2010) define the Critical Zone (CZ) as extending between the tops of the highest vegetation to the top of the unweathered bedrock surface (Fig. 1). The Critical Zone is where most terrestrial organisms reside, and where most non-tectonic terrestrial geomorphological processes take place. This zone of the surface and shallow subsurface typically encompasses the top of at least one unconfined aquifer and where present, the accompanying surface water flow.
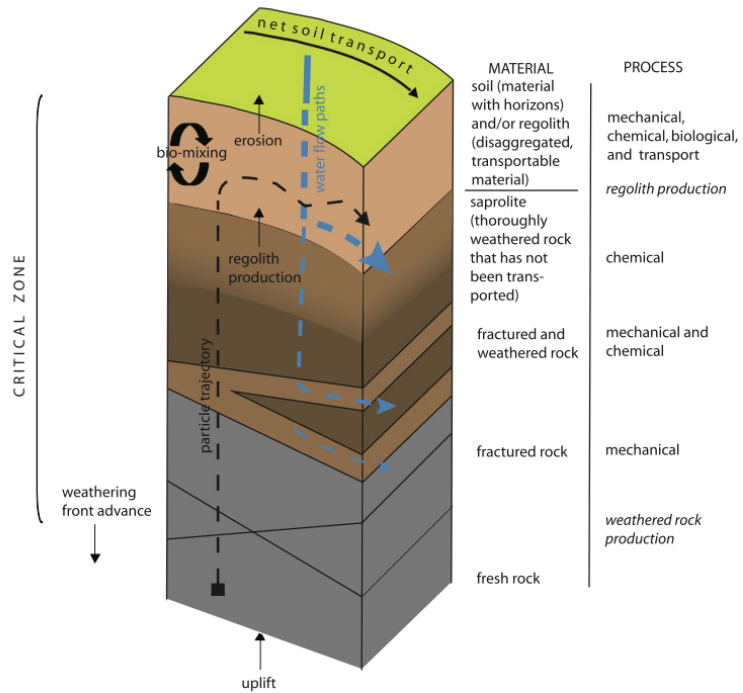
Figure 1. The Critical Zone: infiltrating water aids the advance of the weathering front and surface water aids in the transport of surface deposits (after Anderson and Anderson, 2010).
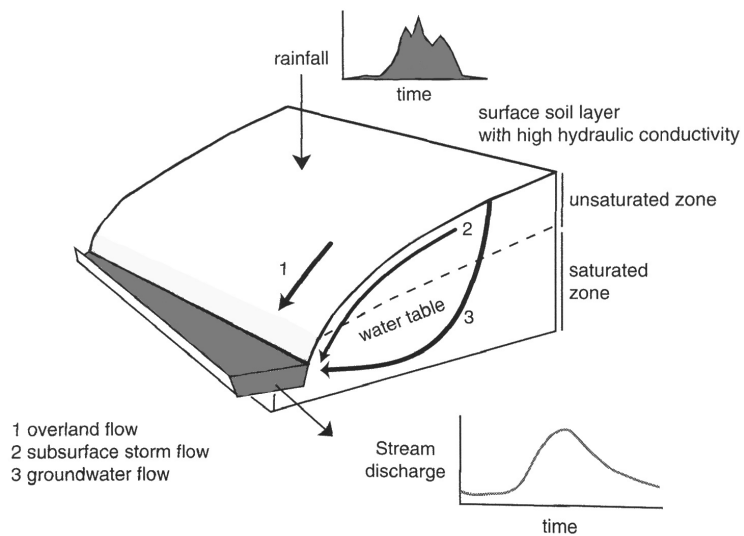
Figure 2. Visualizing simple flow paths during a rainfall event (after Anderson and Anderson, 2010).

Open-channel flow comprises runoff (water that drains from the near surface of an area of land) and groundwater that seeps upwards through the bed of the channel (Fig. 2). Though many of the factors contributing to surface and groundwater flow are the same (and the two interact in areas of hyporheic flow), it is important to distinguish factors related to surface flow, which is easily measured. The factors contributing to and subtracting from surface discharge in a watershed can be additive or subtractive (Fig. 3). Additive factors include: (1) precipitation; (2) melting ice or snow; (3) groundwater storage flux. Subtractive factors include: (4) evaporation (E) from surface water or snow; (5) sublimation from blown or packed snow; (6) evapotranspiration (ET); (7) loss of groundwater to adjacent basins. Blown snow redistribution (8) can alter the snowmelt contribution on a quasi-local scale, depending on the wind direction and topography. I seek to quantify (1) and (2) and to estimate the input/output value of (3) and (7). I estimate (4), (5), (6), and (8) using values from previous studies in the Green Lakes Valley. Snow redistribution due to wind is also an important factor for these basins.
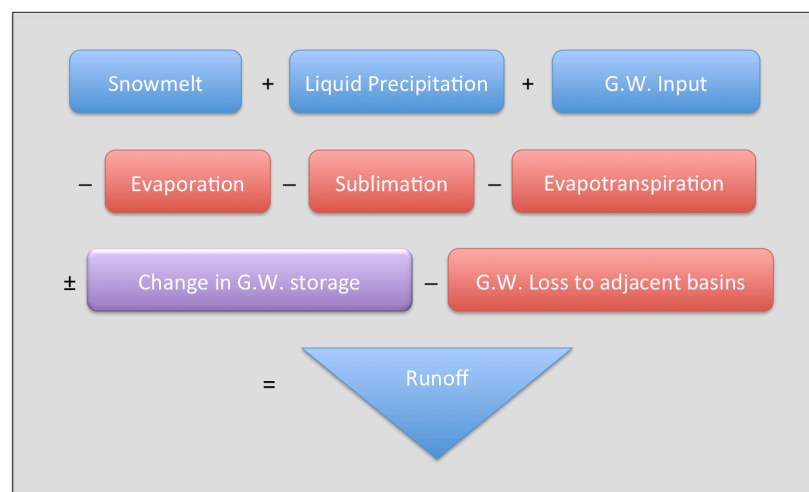
Figure 3. Factors that increase and decrease surface flow (runoff).

Calculating discharge

King (2012) provides background on water budget calculations, and gives an equation (from Scanlon et al., 2002) to calculate a water budget in terms of storage (ΔS^*) in basins. King (2012) modifies this equation to include a separate term for sublimation and removing groundwater evaporation gives the following equation in depth flux units:

$$P + Q_{sw} + Q_{gw} - SL - E_{sw} - ET - Q_{sw} - Q_{gw} = \Delta S_{uz} + \Delta S_{gw} \qquad \text{[Eqn. 1]}$$

where P is precipitation, SL is sublimation, E is evaporation, ET is evapotranspiration, Q is discharge, and S is storage, in mm. Subscripts denote water locations relative to the surface: $_{sw}$ is surface water, $_{gw}$ is groundwater, $_{uz}$ is the unsaturated zone. Modifying Eqn. 1 slightly, I can display the budget in terms surface runoff in alpine basins, and add a value for snowpack melt (Fig. 4):

$$P + P_{melt} - SL - E_{sw} - ET - Q_{gw} - \Delta S_{uz} - \Delta S_{gw} = Q_{gw} \qquad \text{[Eqn. 2]}$$

Q_{in} can be assumed to be zero due to the fact that the basins in question are alpine headwaters regions, and therefore by definition do not have any input other than solid and liquid precipitation (plus drifted snow; Hood et al., 2010).
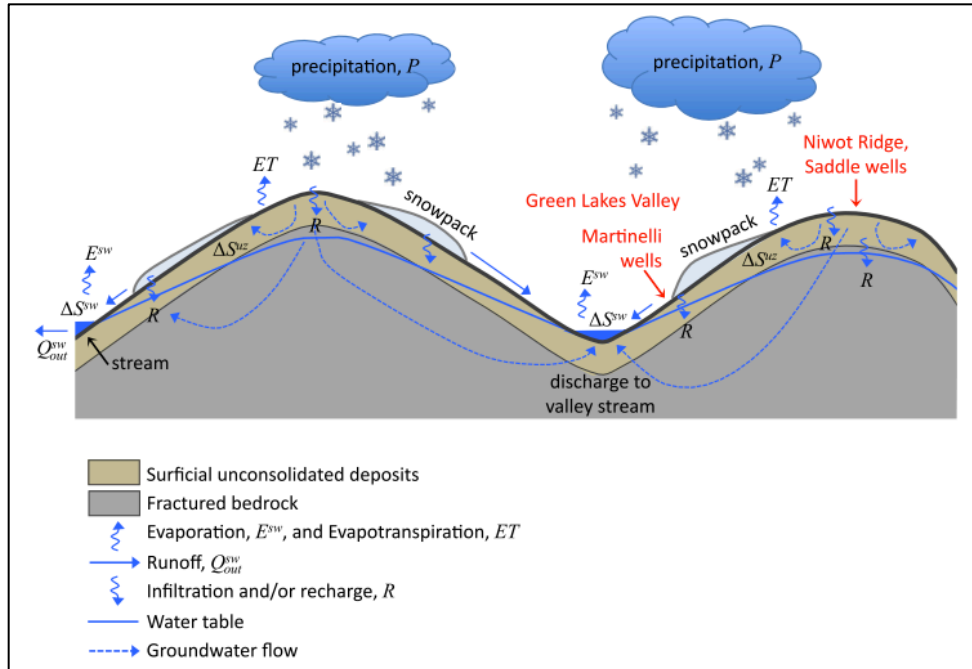
Figure 4. The mountain water budget. Precipitation (P) is the input, including redistributed snow (Hood et al., 2010); evaporation and sublimation (E_{sw}), ET, and flow out of the basin (R and Q) are the outputs. The change in storage (ΔS_{gw} and ΔS_{uz}) also contributes to runoff, although the unsaturated zone of coarse materials probably does not hold much water (after King, 2012).

Factors that contribute to surface discharge in catchments

Precipitation is the total yearly rain and snow (in snow water equivalent, or SWE) that falls in the watershed. Liquid precipitation makes its way to groundwater faster initially than frozen precipitation, which gets stored until warmer months; but once snowpack begins to melt, snowmelt and its contribution to water in the basin vary diurnally. Sheltered areas accumulate significantly more snow in the winter due to remobilization by wind (Hood et al., 2010). Snowpack density increases throughout the late spring, so calculations using snowpack require density.

Rainfall or meltwater falling directly on colluvium (quasi-mobile hillslope deposits) infiltrates to feed groundwater, raising the hydraulic head of the system,

pushing water from areas of high head to areas of low head, and ultimately into a channel or other surface location where the water re-emerges at the surface (Fig. 5).
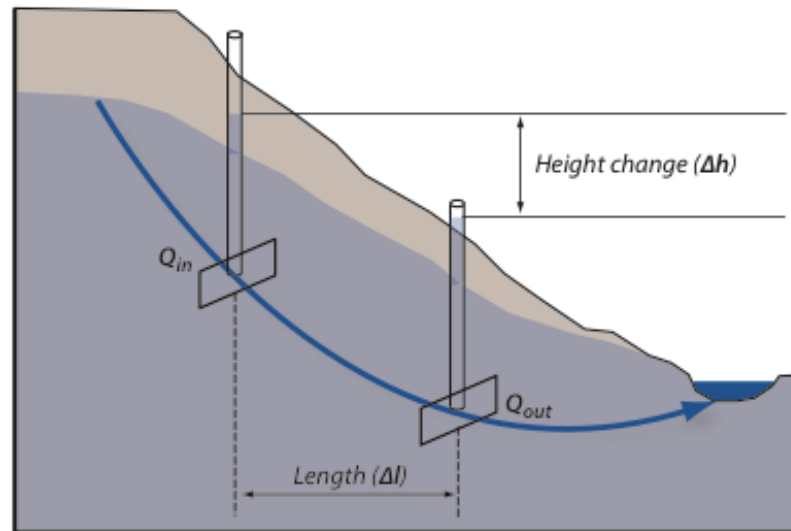
Figure 5. Visualizing simple head change according to Darcy's law (after Bierman and Montgomery, 2013; Darcy, 1856).

In humid areas, this surface expression could be a spring, wetland, stream, river, lake, or other water body. In many cases, streambeds are places where surface water and groundwater interact and exchange freely, in which case they are characterized as hyporheic, or part of the vadose zone (Fig. 6). The area of exchange of these hyporheic zones shrinks and swells depending on the groundwater elevation (how much of the groundwater table is in contact with the stream increases as groundwater elevation increases).
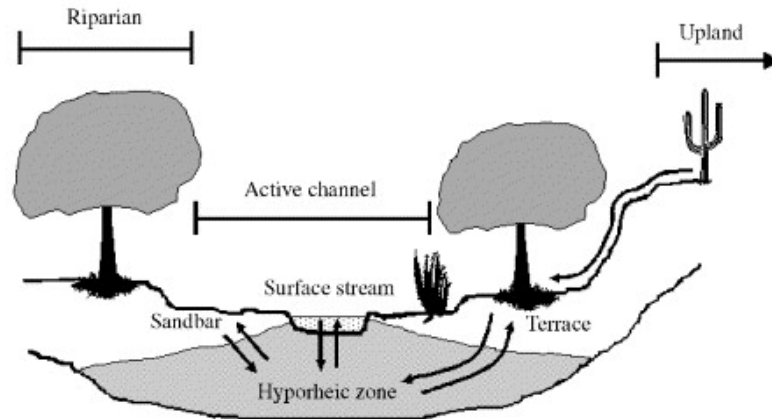
Figure 6. Schematic representation of hyporheic flow in an arid environment (from Fisher et al., 2007).

Since groundwater flow may not strictly follow topographical contours, runoff calculations using watershed boundaries chosen by Geographical Information System (GIS) decision-making engines may not account for groundwater that travels to and from adjacent basins along joints, faults, or bedrock surfaces that do not imitate surface topography.

Factors that decrease surface discharge in catchments

An inherent problem in evaluating snowmelt is that it involves three processes of energy transfer—radiation, convection, and conduction—which have complex relationships with each other and the local and climatic environments in which snowpacks exist. On clear late spring or summer days in exposed areas, solar radiation is the prime factor in melting snow, and convection and conduction can be affected by winds. However especially in heavily forested areas, solar radiation and wind can be obstructed, changing the way snowmelt occurs (Rantz, 1964).

Measurement problems are more numerous when dealing with water. Evaporation is a phase transition that occurs as vaporization from the surface of liquids, and is modulated by many factors, including pressure, temperature, water vapor saturation of the air, and wind speed. In general, evaporative forces are strongest in conditions combining warm water and windy, dry days.

Snow and ice are subject to sublimation (a solid-vapor phase transition) under certain weather conditions. The ideal conditions for rapid sublimation are low temperatures, intense sunlight, and dry winds. However for ice crystals to sublime efficiently, they must have a large surface area to volume ratio. This means that newly formed snow crystals generally sublime most effectively, whereas mature ones are more stable.

Evapotranspiration is the process in which plants take up water from the ground and use it to capture metabolic nutrients. Evaporation (by solar energy) of water transpired through leaf stomata creates a potential differential that causes water to be drawn up, by capillary action, through the plant from the soil. In vegetated watersheds, this process can account for a significant amount of atmospheric water escape during warmer months.

Groundwater/surface water interactions

Essential to this project is the understanding of various flow pathways and surface water/groundwater interactions, which can be complex. In humid regions, flow in channels typically increases downstream by tributary and groundwater input, but that is not always the case. Bierman and Montgomery (2013) visualize surface water flowing through the bed to groundwater in arid regions, and the opposite in humid regions (Fig.

7), which means that surface flow infiltrates to provide groundwater recharge and that surface discharge decreases downstream. In basins where the bedrock surface is undulatory and overlain by unconsolidated material, convex bedrock contours may force shallow groundwater to intersect the surface, feeding surface water. Changes in the thickness of the underlying permeable material can similarly control the amount of underflow in an influent environment (where surface discharge is lost to infiltration into groundwater).
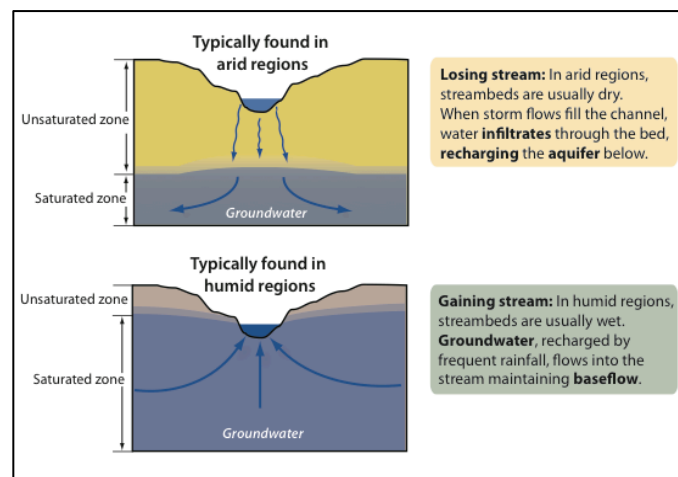
Figure 7. Sketch showing gaining and losing streams (from Bierman and Montgomery, 2013).

Study overview

Annual yield disparity

The essence of the problem addressed is the fact that the hydrological input and output values of the two study sites are significantly disparate (Fig. 7). Precipitation recorded near the basins averages 930 mm yr^{-1} (Niwot Ridge Meteorology and Climatology [NWTMET], 2012) but the discharge totals only about 1/3 of that: 310 mm

yr^{-1} (~33% yield) in Martinelli, and 280 mm yr^{-1} (~30% yield) in Saddle (T. Nelson Caine, unpub. data; NWTMET, 2012).
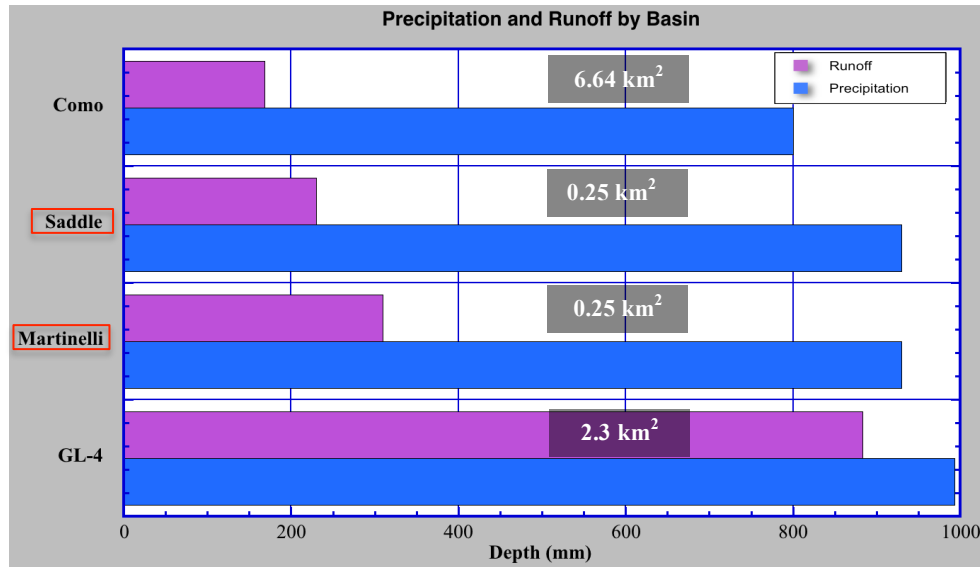
Figure 8. Graphical representation of annual specific yield (runoff) versus precipitation in the study areas. Como has an area of 6.64 km^2, Saddle and Martinelli are 0.25 km^2 basins, Green Lake 4 is 2.3 km^2 (Cowie, 2011; Leopold et al., 2010; NWTMET, 2012; T. Nelson Caine, unpub. data; Caine, 1995a; Greenland, 1989).

Summary and study goals

The amount of water entering a basin must equal the amount escaping. Since known disparities exist between precipitation and measured discharge of the study basins, water must escape by other means than surface discharge. Using known and measured hydroclimatic input and output values, we can constrain the value escaping to attempt to create a comprehensive and predictive water budget. This water budget can serve as a model for similar studies in unglaciated areas, and also as a cautionary example for studies that might use surface discharge as a proxy for precipitation.

The goals of this study are to observe and quantify the disparity in discharge in two alpine basins using synoptic measurements. I also attempt to interpret the Critical Zone hydrology and hydrogeology and hypothesize the cause of the discharge disparity using statistical and geophysical methods, as well as concepts from previous research conducted in the study areas.

SETTING

Location

The Boulder Creek catchment lies in the Indian Peaks Wilderness in the center of Colorado's Front Range at about 40ºN latitude (Fig. 9). It includes three main watersheds: South, Middle, and North Boulder Creek, all flowing east from the Continental Divide. Green Lakes Valley, at the northern end of the North Boulder Creek catchment area, is a broad, recently glaciated U-shaped valley characterized by several bedrock steps and basins, which house the five Green Lakes and Lake Albion. The City of Boulder Watershed area encompasses much of upper North Boulder Creek. To the North of the valley stands a topographically broad, high-elevation ridge separating two U-shaped valleys: the Niwot Ridge interfluve.

Niwot Ridge is located about 35km west of Boulder, and is characteristic of ridges in the Indian Peaks area with, "deep U-shaped valleys separated by long broad interfluves that narrow into arêtes at the Continental Divide," (King, 2012; p. 9). Niwot Ridge and parts of the Green Lakes Valley are the location of the Niwot Ridge Long-Term Ecological Research (NWTLTER) site, which is monitored by various biological, geological, and ecological study groups as the representative North American windswept, unglaciated alpine ridge (Bowman, 2001). One of the most prominent groups studying the site is the University of Colorado at Boulder's Institute of Arctic and Alpine Research (INSTAAR).

14
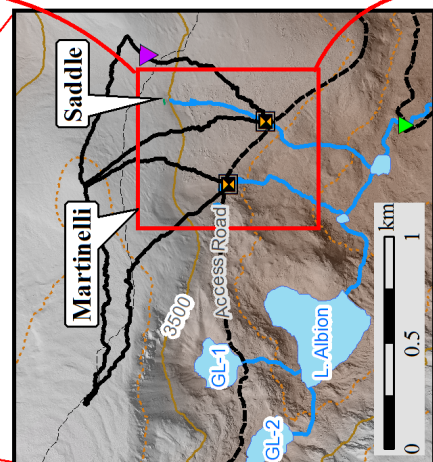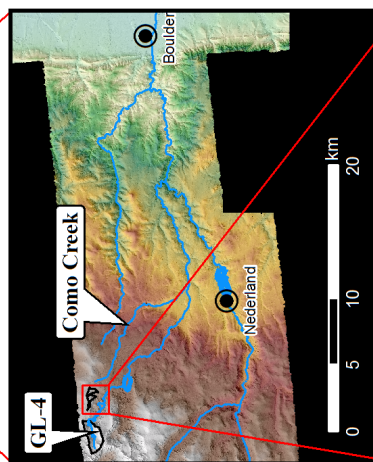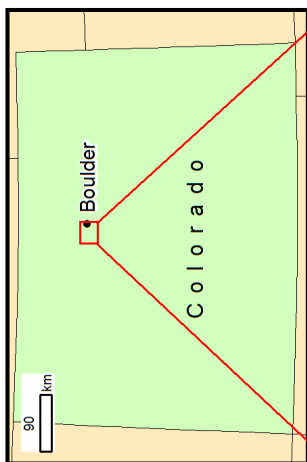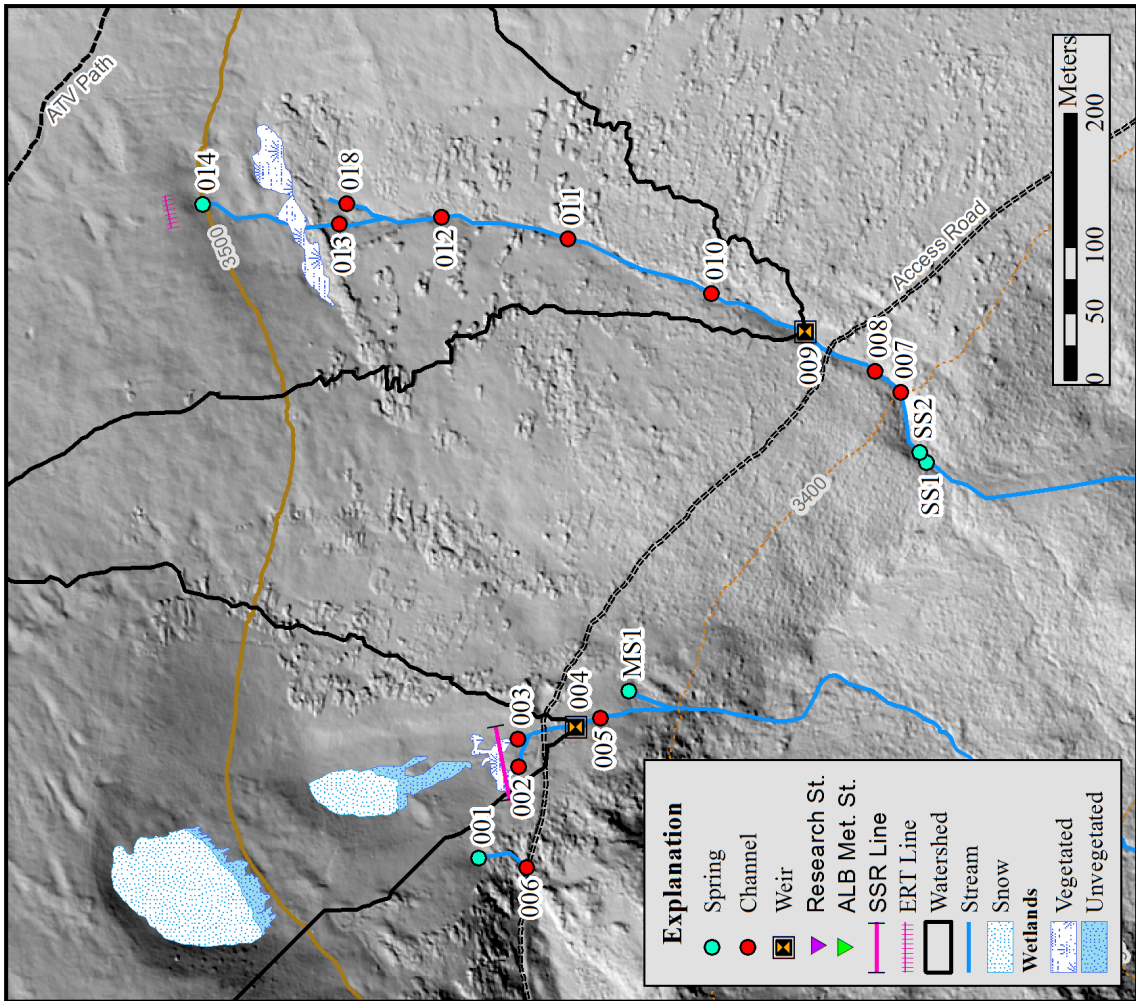
Figure 9 (previous page). Left, from top: location of study area in Colorado, in the central Front Range, and in the lower Green Lakes Valley. Right: lower Saddle and Martinelli basins in detail, with synoptic measurement points indicated and denoted as either spring- or channel-based. LiDAR base is from the Boulder Creek Critical Zone Observatory (Anderson et al., 2012). Contour interval is 100 meters.
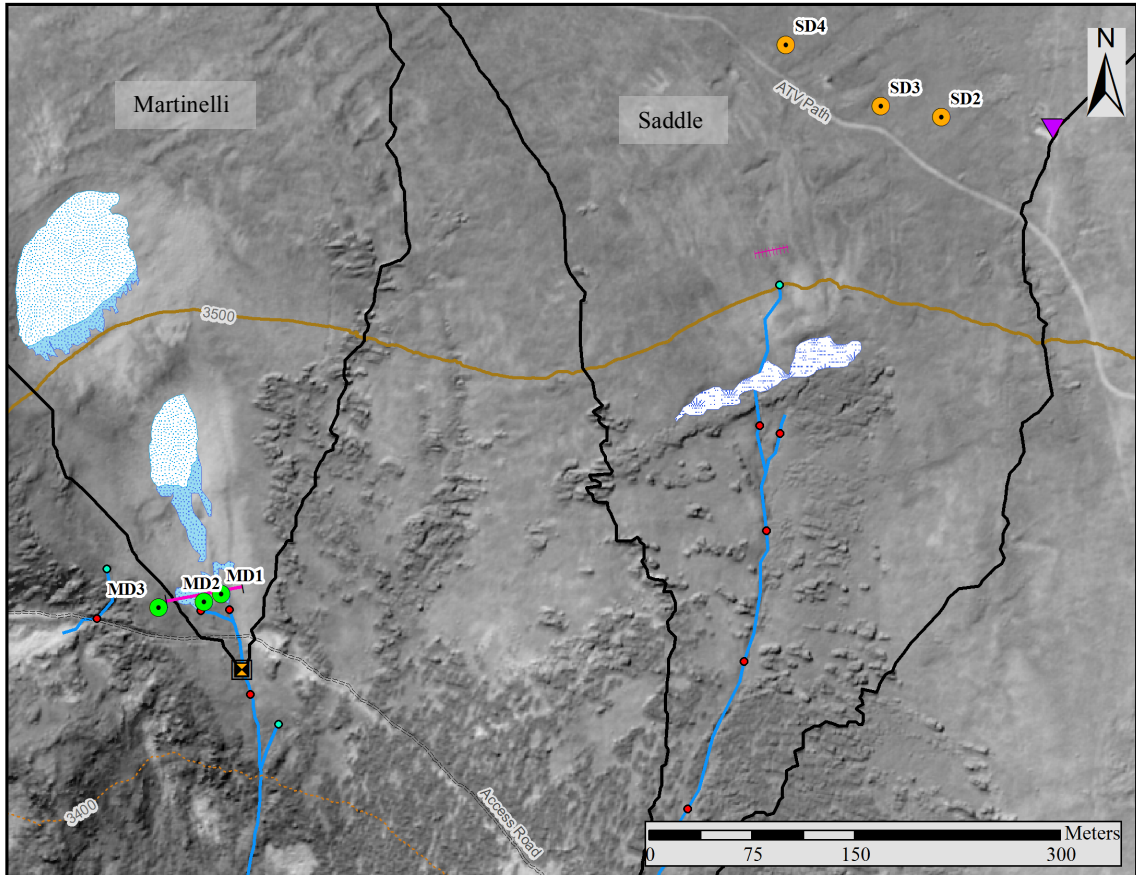
Figure 10. Large-scale view of the basins, with a black and white orthophoto (USGS, 1999) overlaid on LiDAR. Well locations used in Cowie (2011), King (2012), and others are labeled. Other symbology is explained in Fig. 9.
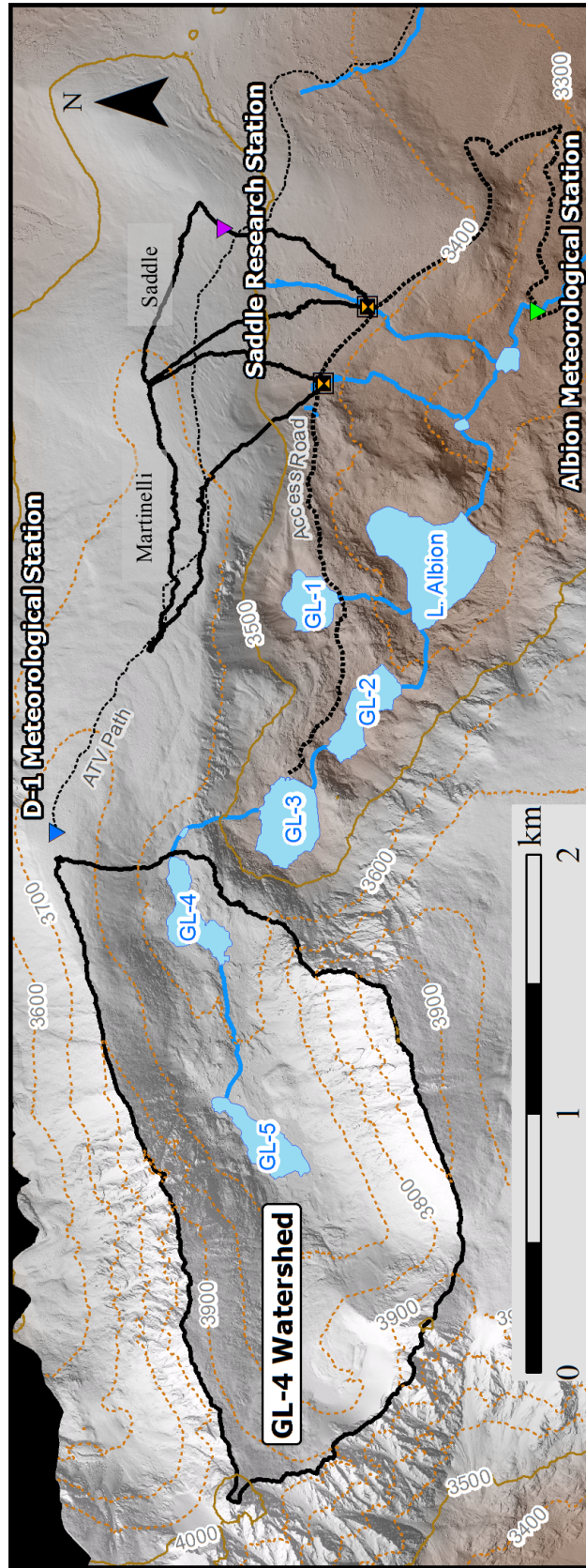
Figure 11 (previous page). The Green Lakes Valley in LiDAR detail, with significant hydrological features, travel routes, and meteorological monitoring stations indicated. Contour interval is 100 m.

There is very little infrastructure near the Niwot Ridge study site, apart from the Tundra Lab and D-1 research and meteorological stations positioned along the top of the ridge (Fig. 9), and the small abandoned mining community of Albion down in the valley (located west of Albion Meteorological Station in Figs. 9 and 11). Bouldery periglacial deposits and currently inactive solifluction lobes dominate the topography and surficial geology of the ridge (Figs. 12, 13). An ATV trail, which researchers use to transport materials to or make repairs on the meteorological structures atop the ridge, winds along the top of the ridge to the D-1 climate station. Compaction may locally affect water transport on the trail surface, especially during high snowmelt and large precipitation events, but otherwise probably does not significantly alter natural water transport. The path is roughly 125 meters north (upslope) of the uppermost Saddle stream measurement site used for this study, and approximately 150 meters north of the edge of the Martinelli snowfield this field season (Fig. 13).
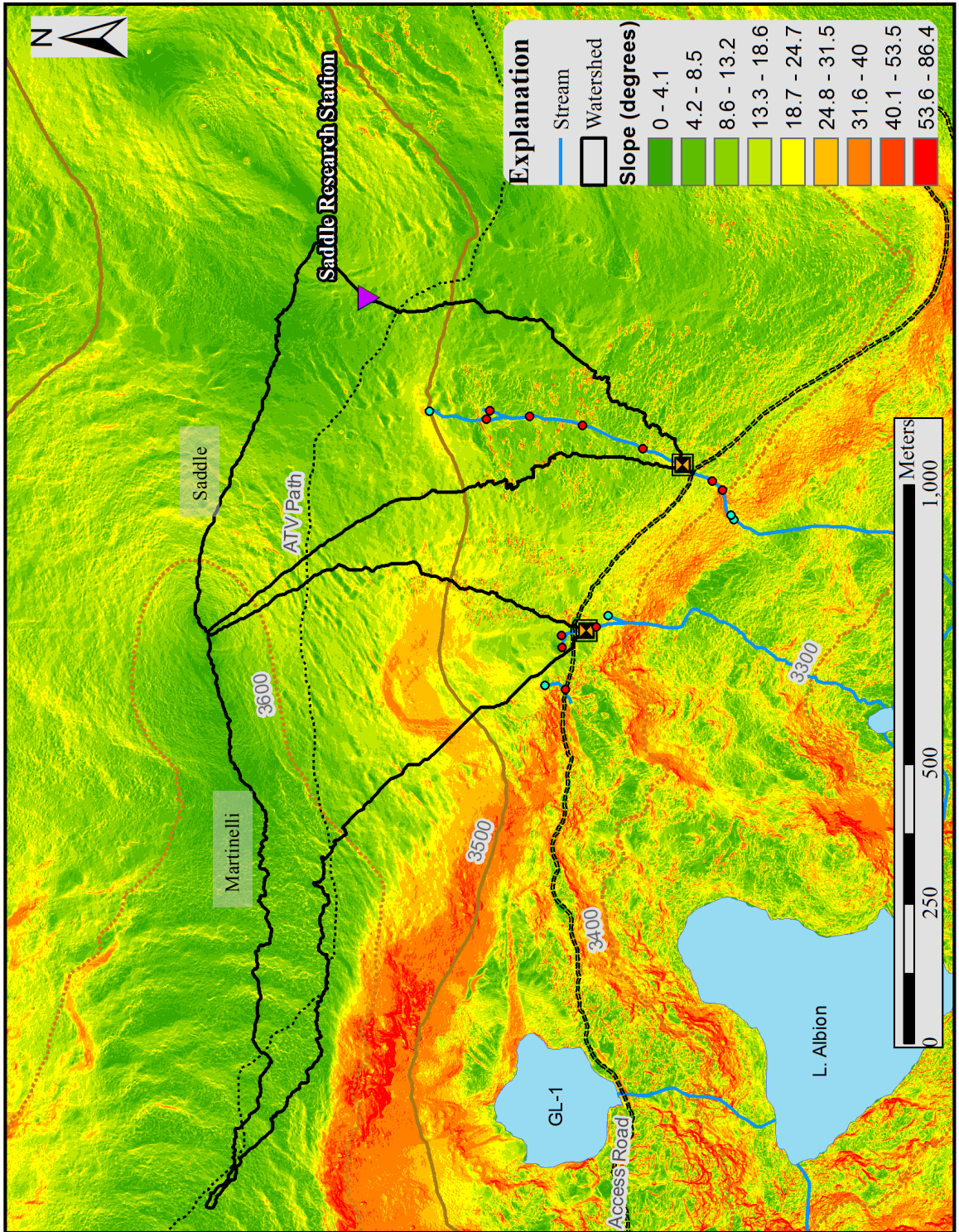
Figure 12 (previous page). Slope map of the basin areas, derived from LiDAR base (Anderson et al., 2012).
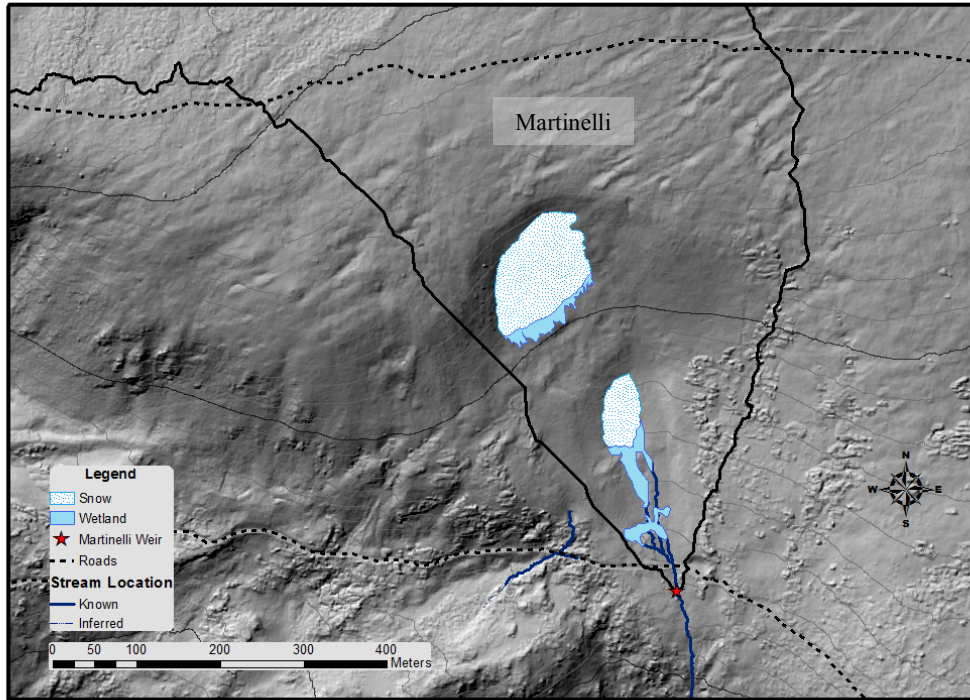
Figure 13. Martinelli snowfields and associated wetland areas (7/10/2012).

Apart from research, the area has been exposed to relatively little human influence in the past century, as mining operation at the Snowy Range Mine (located upstream of the village of Albion, on the south side of Lake Albion), was abandoned in 1910 (Lovering and Goddard, 1950). Since then, the area has become the Boulder city watershed. Several lakes have been dammed to increase water storage for the city, including Albion and Green Lakes 1, 2, and 3 (Fig. 11). An unmaintained, infrequently-traveled service road runs from "downtown" Albion to Green Lake 3, and crosses both the Saddle and Martinelli watersheds, the streams from which locally run in the tire ruts for a few meters (in the case of Saddle stream) or a few tens of meters (in the case of

Martinelli stream). This road is used for flatbed access to the study sites and by the City of Boulder Watershed division.

Measurement stations

Several NWTLTER measurement stations exist near the study areas. The most significant of these are C-1 and D-1 climate monitoring stations (see Fig. 9), which each have been in operation since the 1950s (Bowman, 2001). The Tundra Lab meteorological station also houses significant climate monitoring instruments and features a webcam (instaar.colorado.edu/tundracam/view.php). Monitoring stations at Albion and Green Lake 4 feature streamflow gages, and although data from them is not generally available, T. Nelson Caine was generous enough to lend me access to them. Other nearby climate monitoring sites include two National Resources Conservation Service (NRCS)-run stations: University Camp station (U. Camp), near the watershed manager's residence at Silver Lake (1978-present), and Soddie, near C-1 and the Mountain Research Station (1979-present). Up-to-date climate records, however, have not been readily available for the NWTLTER sites, and therefore the recent data used for this study comes from both the National Resources Conservation Service's University Camp climate station (or "U. Camp," approximately 2.5km south at 3139m) and INSTAAR's Albion climate station (0.8km south at 3261m).

Saddle stream site

Saddle is a small basin (0.25 km^2 at the installed weir; only a few hundred more square meters at the lowest measurement sites) on the south face of Niwot Ridge,

downslope of the Tundra Lab. The Saddle stream is ephemerally intermittent over distance, and like its nearby counterpart Martinelli, can stop flowing entirely in places towards the end of the melt season. After the small snowfield disappears, the stream is most likely fed in part by ice lens, frost, and/or permafrost-derived melt input from upslope. Surface flow in the catchment starts at small springs nestled into a break-in-slope that accumulates a small snowfield near the top of the ridge (Fig. 14).
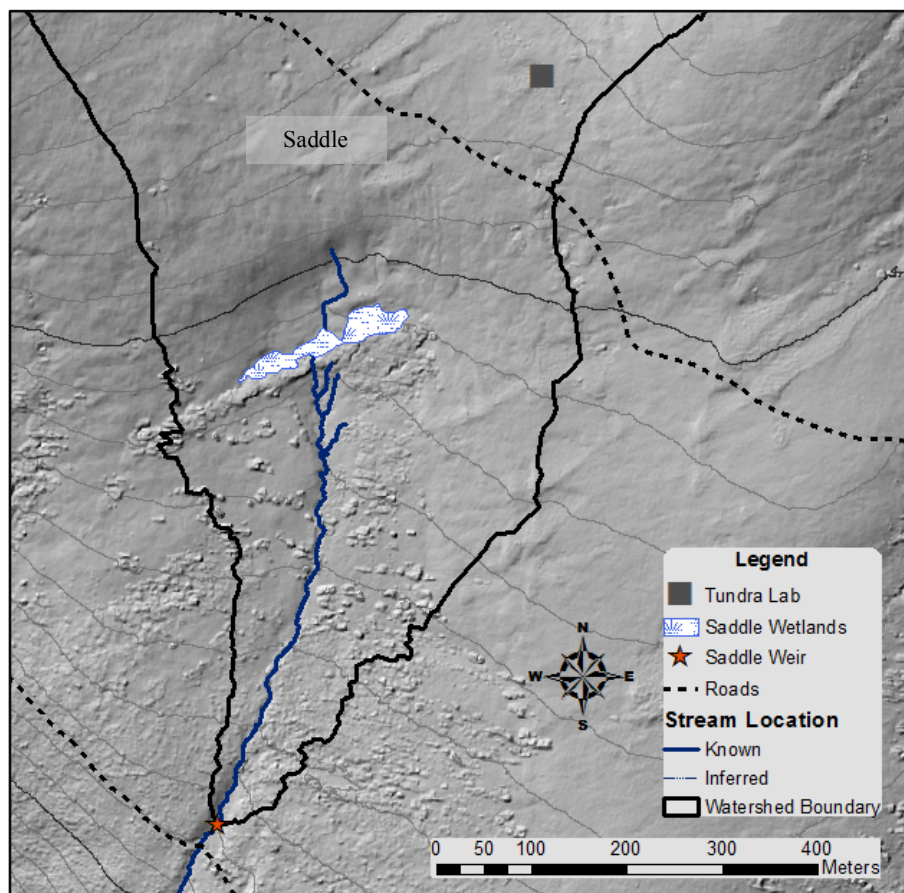
Figure 14. The Saddle stream, with weir and associated wetlands.

The Saddle wetlands are locally quite flat, densely vegetated, and host an area of stagnant water year-round (Fig. 15). Among other things, alpine grasses, Barrenground

Willow (*Salix brachycarpa*), various mosses, and low, broad-leafed angiosperms make up much of the area's megaflora. At the wetlands, dense stands of *S. brachycarpa* take advantage of the high moisture content of the surface material. Many of the *Pinus monticola* (White Pine) that populate the bottom of the Saddle catchment at treeline are heavily flagged towards the east (meaning that their growth has been stunted due to strong west winds in the winter). The Saddle wetland persists long after the overlying snow has melted, and is fed by summer rainstorms and groundwater from upslope.

Figure 15. The Saddle wetlands, looking downslope from near the uppermost emergence of the stream.

Hydrology

Saddle stream is equipped with a pressure transducer at its weir, which takes measurements every 10 minutes during the melt season. Flow in the basin is strongly diurnal during the early period of the falling limb of the hydrograph (Fig.).

The Saddle watershed has four monitoring wells positioned on the ridge near the Saddle Tundra Lab Research Station (purple "Research Station" indicator in Figs. 9–11). Three of these wells are hydrologically relevant and have good post-hydrograph peak (or post-peak) correlation with discharge measurements over the period 2006-2012 (Fig. 35). In a representative year, the melt season time series (Fig. 16) shows a lag-to-peak period likely related to the permeability of material that the wells were drilled in.
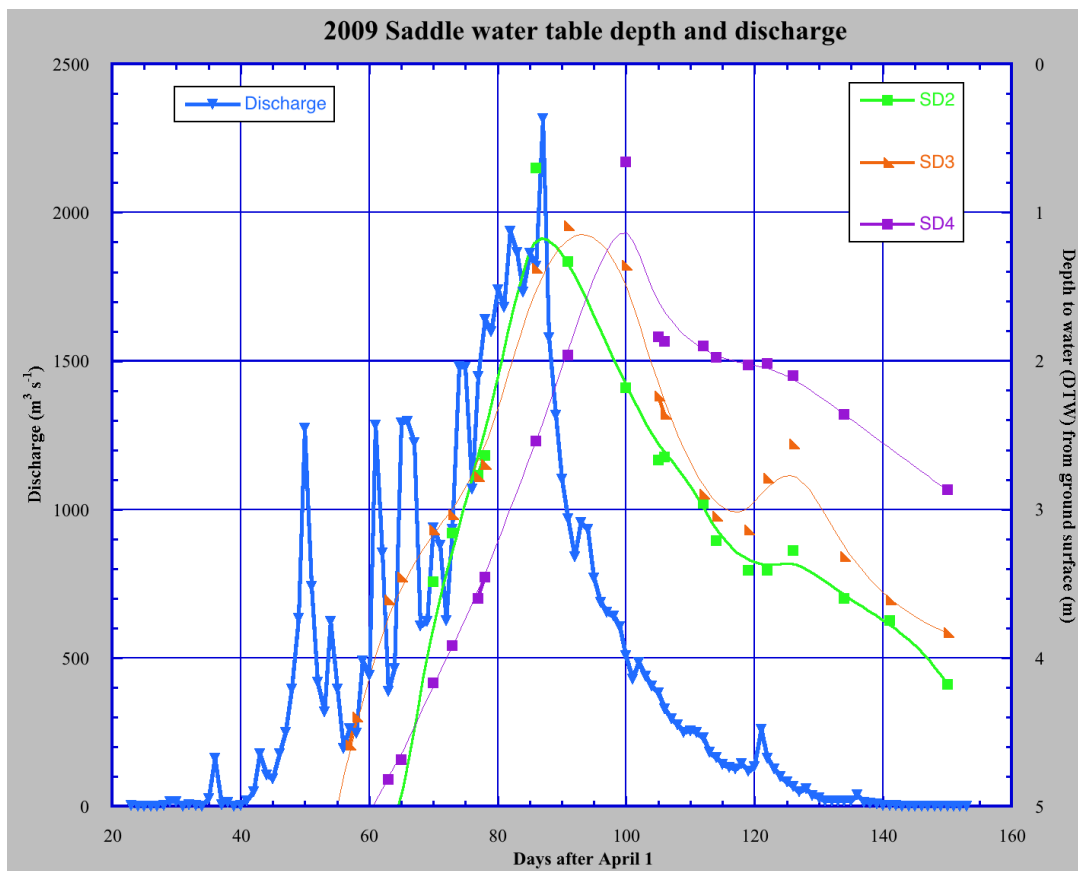
Figure 16. Discharge and water table depth in Saddle basin over the 2009 melt season (well locations are shown in Fig. 10). The graph is a time series of discharge in m³d⁻¹ (blue) and distance to water from ground surface in meters at SD2 (green, 3509.6 m elevation), SD3 (orange, 3510.7 m elevation), SD4 (purple, 3518.8 m elevation) over the 2009 melt season. Note the lag-to-peak in water table elevation at individual wells, which suggests that they are drilled in material of different permeabilities, are on different flow paths, or (most likely) both. Smoothed lines do not represent water table depth, they simply serve to highlight general trends.

Previous studies

Although Dr. Nel Caine maintains a record of discharge and water chemistry for Saddle stream and multiple studies have focused on aspects of the nearby Martinelli basin, much less has been published about Saddle stream. In the past few years, three masters and undergraduate theses (Cowie, 2011; King, 2012; Winkler, 2012) have examined the hydrology, hydrogeology, and hydrochemistry of parts of the Saddle stream, but none of these studies focused exclusively on water budget or implications for alternate flow pathways. Cowie (2011) investigated snowmelt hydrochemistry and groundwater at the top of the Saddle catchment and at several other locations, including one at "Soddie" near Como Creek, just east of Saddle basin. He did not use discharge measured at the Saddle weir. King's (2012) study is strictly based in the Saddle and Martinelli watersheds, but she also focused on groundwater. Her work is also mostly based at the top of the Saddle catchment, and she uses the same wells that Cowie (2011) cites in his study. Winkler's study focused on discharge and stream chemistry measurement in these basins. His study was shorter and not quite as in-depth as the other two, but it provided insight and comparison of hydro- and geochemistry between the two basins that had previously been poorly understood, if at all. Winkler used discharge data from NWTLTER and Dr. Nel Caine, but his measurements were taken at the gage only.

Martinelli site

Although the sites are similar in size (Martinelli basin is 0.255 km^2 above the weir) and not more than a few hundred meters apart, they are distinct in their processes of

accumulation of snow and their small-catchment hydrology. Despite the fact that Martinelli is a bsain around the same size as Saddle, and at similar elevation (3410m at the weir), Martinelli has a snowfield that persists much later and a morphology and directionality that make it a nivation hollow. The snowfield melted completely during roughly half of the years from 1982-2012 (Caine, unpublished data).

The calculated area for Martinelli basin using the Watershed tool on filled LiDAR data in ArcGIS may be slightly larger than the true hydrologic catchment area; an elongated extension of the basin located northwest of the main basin area, which is underlain by layered periglacial deposits, is located directly above a 200 m long section of cliff that may provide a more proximal hydrologic outlet. The cliff is nearly vertical at the top, has likely been undercut in a recent glacial event, and is composed of bedrock. It is visible on LiDAR approximately 500 m west of the snowpack. It is not known whether or not this extension is truly hydrologically connected to the Martinelli watershed. Given the surficial geology and inferred porous hydrologic characteristics of the shallow subsurface, the water likely escapes the bounds of the calculated extent in the northwest corner of the Martinelli watershed.

Figure 17a (previous page). Looking west at the middle of Martinelli watershed with and b. without snowfields (7/19/2012 and 8/7/2012). Note that the "wet skirt" of snowmelt-

saturated hillslope deposits ends not far below the snowpack itself as snowmelt disappears completely into the subsurface.

West wind is an important factor for the buildup of the Martinelli snowfield (Fig. 17) during the months in which nivation (snow accumulation) dominates. Because of its south-southeasterly aspect and locally steep slopes, the Martinelli basin's nivation hollow captures a large amount of drifting snow from northeast winds during and after snowstorms that scour the top of the ridge. The depth of the late spring snowpack at this location is the main factor for the late-lying nature of this unusual south-facing snowfield.

Due to the permeability of the hillslope deposits the snowpack lies on, all the snowmelt from the upper Martinelli snowfield disappears into the subsurface within 20 m of the lower edge of snow extent, and no water reappears for more than 100 m downslope (Figs. 17, 18).

Because many years it is exposed late in the growing season, the area adjacent to the Martinelli snowfields is nearly unvegetated. Grasses and broad-leafed angiosperms provide surround the snowfield areas and make up a large portion of the riparian areas around the stream. A small stand of ~40-60 *Pinus monticola* exists in the lower right side of the watershed.

Figure 18. Gabe Lewis near the Martinelli stream gage (out of frame left). Note that from this angle, hillslope deposits below the upper snowfield do not appear saturated. Because of the permeability of the material it flows over, snowmelt travels less than 20 m downslope of the snowpack on the surface before it enters the subsurface.

Previous studies

Two individuals in particular spearheaded past research in the Martinelli basin. The first is its namesake, M. Martinelli, Jr. His interest in increasing alpine storage of freshwater drove him to conduct several studies in which he uses snow fences to attempt to promote greater deposition in the hollow. Martinelli (1959) provides detailed observation of summer hydrologic conditions in the basin. Dr. T. Nelson Caine continues to provide significant and widely cited research on the Green Lakes Valley in general. Caine's independent works referring specifically to the Martinelli catchment are numerous (Caine, 1989a; 1989b; 1992a; 1992b; 1995a; 1995b), and he maintains an intimate knowledge of the site and a large store of unpublished data.

A few studies focus at least partly on geological or hydrological aspects of the basin since the beginning of the last decade. Clow et al. (2003) investigates groundwater contributions to the streamflow of the basin. Liu et al. (2004) provides evidence to support a flow path model for snowmelt. Leopold et al. (2008) uses geophysics to create a cross-section and examine the composition of the subsurface material downslope of the snowfields.

Masters or undergraduate thesis students have amassed a relatively significant collection of work on the basin in just the last three years. These students are associated either with INSTAAR or with the Keck Geology Consortium and the Boulder Creek Critical Zone Observatory (BCCZO). Parman (2010) investigated stream chemistry. King (2012) used stream chemistry to examine hydrology in both Martinelli and upper Saddle basin. Similarly, Winkler (2012) examined hydrology through the lens of hydrogeochemistry.

These last three theses highlighted the need for a water budget study in both Saddle and Martinelli basins, because it seems as though a significant amount of water leaves the basin without being recorded by the gage. I seek to establish this budget in order to estimate the amount of water that escapes the gage at a given stage of snowpack melt.

Hydrology

Caine (1992b) divided the flow season in Martinelli stream into three segments according to the behavior of diurnal flow at the gage. Prior to the date of peak flow, diurnal periodicity is weak and does not show up throughout the record. After peak flow, the signal is consistent and clear in the record. When the snowpack melts out and surface flow ceases to reach the gage, the record loses all periodicity and "responds only to a declining groundwater contribution and to ephemeral inputs from rainstorms," (Caine, 1992b). Caine hypothesized that any periodicity in the first stage is mostly caused by isothermal patches of snow near the edges of the snowpack, and the second stage periodicity is caused by strong radiative input to the system during the early summer. After peak flow, discharge in the central channels in Martinelli appeared to be directly or quite closely related to snowpack size.

As Caine (1992b) mentions, Martinelli is a losing stream at low-flow points in the year. Discharge is closely tied to snowpack area (and therefore meltwater abundance) and these low-flow periods occur mostly when the snowpack fully melts out. A study published by Liu et al. (2004) found a similar progression of changes in flow paths to that described in Caine's hydrograph studies. The study explains why Caine finds that diurnal flow becomes much more difficult to detect near the end of the falling limb of the

hydrograph: meltwater becomes "baseflow," (shallow groundwater flow) and its travel

speed is reduced by the material it travels through.
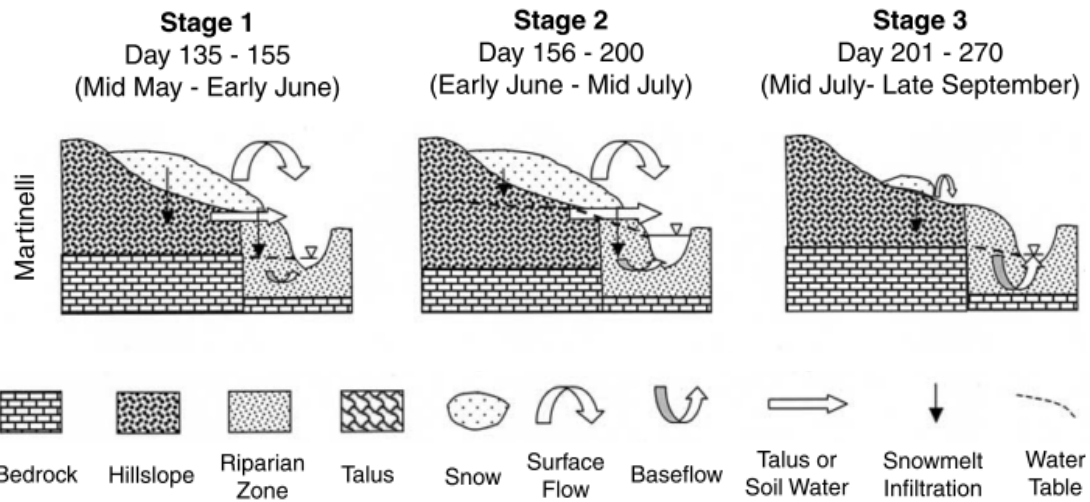
Figure 19. Interpretation of flow paths in Martinelli basin (after Liu et al., 2004). The processes by which water gets to the channel change over time, in a progression that affects the hydrograph. In the rising limb (Stage 1), meltwater flows overland locally and in the shallow subsurface. In Stage 2 (at or near peak flow), water flows increasingly in shallow groundwater pathways. In the final stage (end of the falling limb), flow travels largely as groundwater.

Further pertinent information

Climate and water budget

Both the Saddle and Martinelli drainage basin outlets are located near treeline and

therefore lie mostly in the "alpine" climatic and morphological zones. Martinelli basin

barely contains any tree vegetation (Fig. 10), but because the basin outlet is at about 3420

m, it is technically at treeline. The D1 (approximately 2.1km northwest at 3750m, Fig.

11) and Saddle Research Station (at the top of Saddle stream's watershed at 3527m, Fig.

11) meteorological data (Fig. 9) provide local measurements of the climatic conditions at

the study sites, and further up-valley at Green Lake 4. According to a near 60-year

dataset ending in 2010, Saddle's Tundra Lab meteorological station had recorded a yearly mean temperature of -2.2ºC and 930mm of mean precipitation (NWTLTER, 2010). As much as 80% of annual precipitation falls as snow (Caine, 1995a). This snow comes from storms carried in by a generally northwesterly airflow in the winter or by upslope easterly winds in the spring. Storms that develop due to strong atmospheric convection bring rain or hail during the warm summer months. Average wind velocity at D1 is 8 m/s, with gusts to 50 m/s in the most extreme conditions. Winter winds prevent snow from accumulating on top of the ridge, but can also cause snow to accumulate in shelter provided by hollows like Martinelli and slight lee areas like the one that hosts the Saddle wetland.

Studies of sublimation and ET on Niwot Ridge have focused on the area near the Tundra Lab. The flatter terrain on top of the Saddle ridge supports more standing water, higher winds, and therefore more E than Martinelli. No studies of evaporation have been done lower down on the flanks of the ridge. Due to the absence of standing water on the ridge slopes, E values at the Saddle Research Station may overestimate evaporative losses on the slopes. Table 1 provides a summary of the water budget input and output values at locations at or near Martinelli and the Saddle stream, including both Green Lake 4 (GL-4) and Como Creek (Fig. 9).

Precipitation values can differ greatly over short distances in the alpine zone, so we choose to average two sites (the D-1 station and University Camp at Silver Lake) near the catchments to obtain a more representative estimate for precipitation. Sublimation has been calculated using eddy covariance techniques to interpret wind speed and humidity data from the Saddle Tundra Lab. ET could be as much as 260 mm yr^{-1} below treeline,

but all of Martinelli and most of Saddle basin is above treeline. Most of Martinelli's basin

floor lacks vegetation because of the seasonal snowpack. Knowles et al. (2012) estimate

combined sublimation and E to equal 39% of total yearly precipitation (~360mm yr^{-1})

atop the ridge, but ridgetop measurements differ from those on the slopes because

standing water in wetlands is subject to much greater wind speeds than does water in

slopeside channels. Subtracting Hood et al.'s (2010) estimate of sublimation (15%) from

the total Knowles et al. (2012) value (39%) gives a standalone estimate. Runoff at Saddle

and Martinelli streams is calculated using flow measurements at each of the weirs (Caine,

unpublished).

Table 1. Summary of hydroclimatic values from Niwot Ridge and nearby locations (after King, 2012).

Basin	Elevation (m)	Precipitation (mm)	Sublimation (mm)	Evapotranspiration (mm)	Evaporation (mm)	Runoff (mm)
Saddle	3420	930	*140*	*0 - 260*	*0 - 223*	230
Martinelli	3428	930	*140*	*~ 0*	*0 - 223*	310
Como	2910	800	*140*	*0 - 260*	*0 - 223*	168
GL-4	3515	993	*140*	*~ 0*	*0 - 223*	883

Values expressed in millimeters unless otherwise noted. Italics indicate estimate. Range describes spatially variable value.

Runoff is based on gage records, 1982-2012 for Martinelli and 1999-2012 for Saddle, from Caine (unpublished data), and NWTLTER (2012); 2009 for Como from Cowie (2011); and 1981-1993 for GL-4 from Caine (1995). Precipitation is from NRCS (2010) at Saddle and Martinelli, Leopold et al. (2010) at D-1 for GL-4, and Cowie (2011) for Como. Sublimation is from Hood et al. (2010), ET is based on Greenland (1989), and evaporation is based on Knowles et al. (2012) and Hood et al. (2010). Elevation of Como and GL-4 are from Cowie (2011).

Bedrock geology

Precambrian metasedimentary rocks and slightly younger granitic intrusions

underlie most of the Green Lakes Valley (Gable and Madole, 1976; Cole and Braddock,

2009). Niwot Ridge is composed of one or of several Cretaceous to Paleogene granitic

bodies with slightly varying composition intruding Precambrian gneiss and Granite of Long's Peak (also known as Silver Plume Granite).

According to Gable and Madole (1976), Saddle stream is underlain by a contact between Paleogene quartz monzonite to the west and Precambrian quartz monzonite from the Granite of Long's Peak to the east. It is possible that the contact between the two intrusions is important in the stream's general morphology, as shown in King's illustrative interpretation of borehole data (Fig. 20), however there are no other data to substantiate this claim.
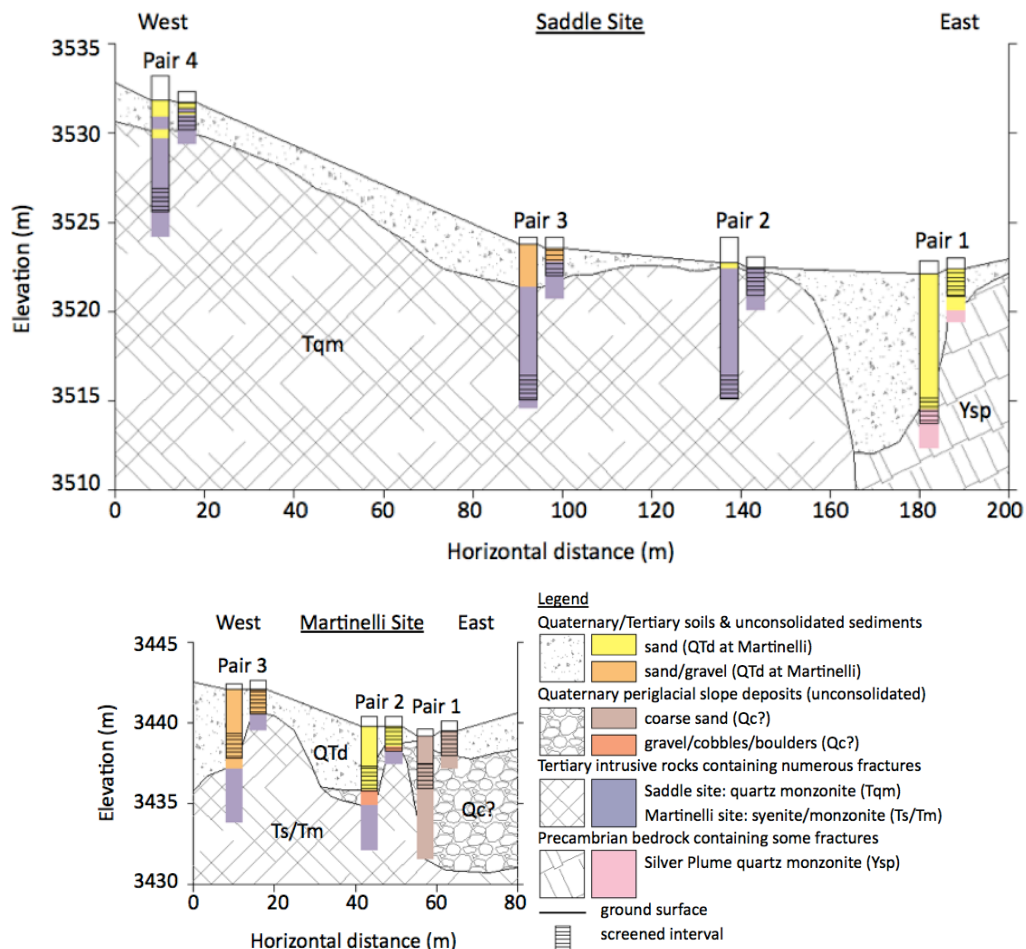
Figure 20. Saddle and Martinelli borehole data (4x vertical exaggeration). Martinelli wells were drilled in wetlands approximately 25-30m above the road, and Saddle wells were drilled near the Tundra Lab, about 100m above the emergence of the Saddle stream (after King, 2012).

Gable and Madole (1976) portray Martinelli basin as being underlain partially to the west by Tertiary/Pleistocene diamicton and partially to the east by Paleogene syenite. Cole and Braddock (2009) list the diamicton deposit in the west side of Martinelli basin as Pliocene gravel. Gable and Madole indicate that the unconsolidated diamicton deposits on the west side of the site have been moved by solifluction. Interestingly, Madole points out that the composition of diamicton debris closely resembles those of tills in nearby valleys and believes they represent either glacial or fluvial deposits from long before Bull Lake time (Gable and Madole, 1976). Madole (1982) rules out glaciation as the source of the diamicton, but does not rule out alluvium, colluvium, and debris flow contributions to the formation of the deposit.

Glacier extent at the Pleistocene last glacial maximum (LGM) in this area is mapped (see Kantack, 2011), but is difficult to identify locally. It is most commonly placed below the access road in both Martinelli and Saddle basins (Fig. 21, Gable and Madole, 1976). Material more than a few tens of meters above the road at these areas is thought to be periglacial rather than glacial in origin, meaning most significantly for this study that there is no latest Pleistocene till layer in the subsurface. The Bull Lake glaciation may have covered more area; Gable and Madole (1976) indicate that the till from Bull Lake time may extend to nearly 100m above (north of) where the Green Lakes access road crosses the Saddle stream, and more than 50m above the road in Martinelli basin. However, no till layer was discovered in the well logs described by King (2012). A closer study of how high this till reaches locally is important to better understanding the interactions of groundwater and surface water in these catchments.
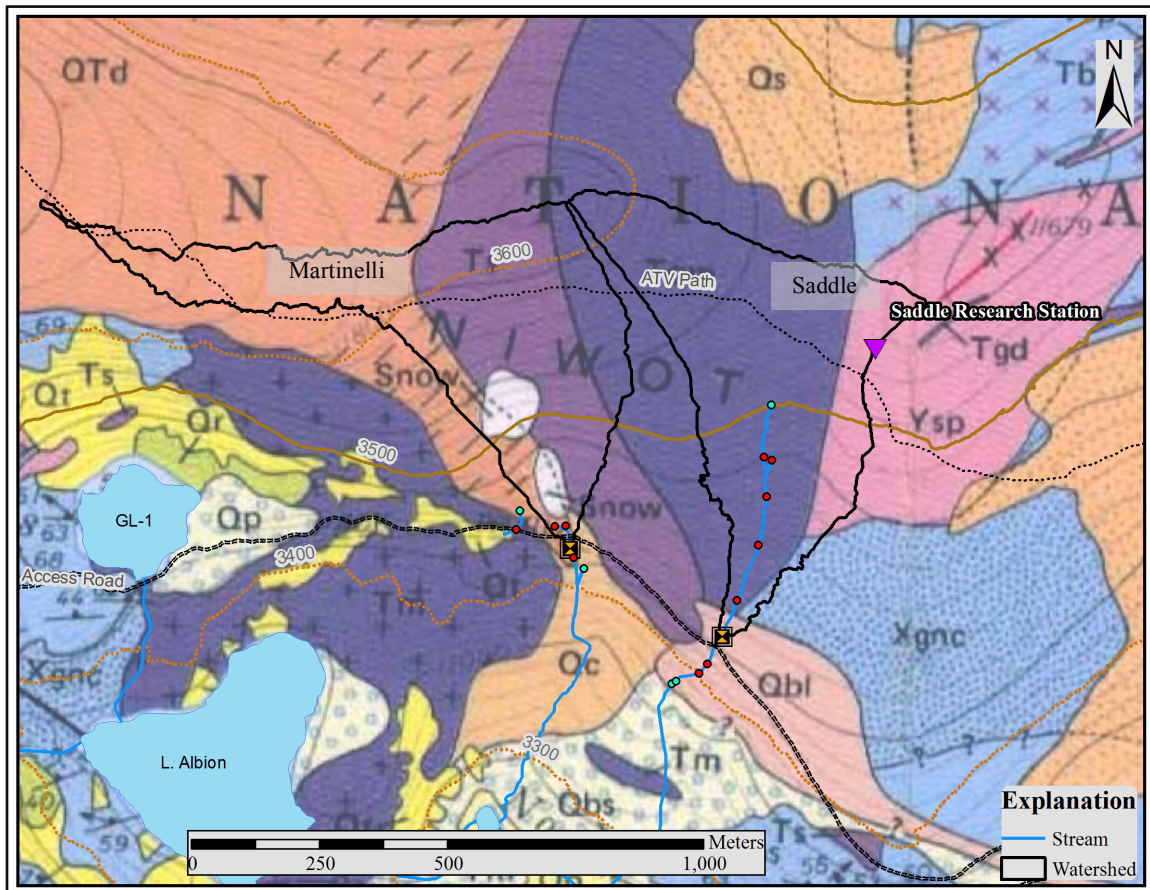
Figure 21. Geologic units in the study area showing the outline of the two catchments (after Gable and Madole, 1976). Select unit abbreviations are: QTd (orange): Tertiary or Quaternary diamicton; Ts: Triassic syenite; Tqm: Tertiary quartz monzonite; Ysp: Late Precambrian Long's Peak Granite (aka. Silver Plume quartz monzonite); Xgnc: Middle Precambrian cordierite-bearing garnet-sillimanite-biotite gneiss; Qc: Holocene colluvium; Qbl: Till of Bull Lake age (Upper Pleistocene).

Surficial geology and subsurface geophysical measurements of Saddle basin

A detailed study of surface material was conducted by Leopold et al. (2008) in upper Como Creek, a basin east of Saddle basin (known as Niwot Trough in the paper). Material described as being "unconsolidated" is found at that site to be more than 1m deep nearly everywhere that the SSR and GPR tests were run.

A few tens of meters above the Saddle stream, borehole data from King (2012) show similar subsurface material composition to that found in Leopold et al.'s (2008) study (Fig. 20). The data provide some evidence about the geological layers above the site that convey groundwater to the springs that begin the stream. The most significant difference between these two studies is the interpretation of the shallow subsurface material. Leopold et al. interpret the shallow (< 2m) subsurface material as an unconsolidated soil, with a layered fine component thought to be eolian. King finds medium sand to gravel to be the predominant size fraction at both sites. Differences in these interpretations, along with those by Gable and Madole (1976), highlight both the heterogeneity of the sites and the difficulty of classifying these deposits. Infiltration investigations have been done (Hamann, 2002; King, 2012) but the surface material of these sites varies so widely that it is difficult to settle on any particular infiltration value. According to King (2012), soil infiltration rates on the flat portion of the Saddle ridge near the wells (Fig. 10) range from $2.87 * 10^{-5}$ m s^{-1} to $3.41 * 10^{-4}$ m s^{-1}, and near the Saddle weir were measured at $1.15 * 10^{-4}$ m s^{-1}.

Surficial geology and subsurface geophysical measurements of Martinelli basin

Although Gable and Madole's (1976) study reports a mixture of bedrock and mobile hillslope deposits below Martinelli basin (Fig. 21), the surficial geology is much more complex than a 7.5-minute geologic map can show. Solifluction and other periglacial processes have locally altered the landscape and shallow subsurface significantly and must play a role in the hydrogeology of Niwot Ridge.

We are fortunate to have both shallow seismic refraction (SSR) data from Leopold et al. (2008) at the Martinelli well site and borehole data from King (2012).

Leopold et al. (2008) calculate composition of subsurface material based on a three-layer model (organic-rich soil and unconsolidated material, periglacial slope deposits including rock fragments and boulders, and bedrock). SSR measures various wave transmission speeds using a point-kinetic energy source and several strategically placed "geophone" sensors to measure the refraction of the wave off of the different subsurface layers. A computer then compiles and processes the data to create an image showing the velocity of the shallow subsurface material.

A 91m-long SSR line about 40m north of the road in Martinelli basin shows that bedrock is fairly deep (3-4m) across the center of the seismic line, and even deeper (4-11m) towards the edges, where a periglacial deposit underlies the surface material (Leopold et al., 2008, Fig. 22). King (2012) interpret the borehole data differently, claiming that lenses of Quaternary colluvium (Qc in Gable and Madole, 1976) exist beginning at 2-4 m depth beneath the east side of the basin, and extend all the way to bedrock. The ~5m of "unconsolidated material" near the surface in Martinelli basin mentioned by the Leopold study could play host to a significant amount of water, depending on its permeability, as could the layer interpreted as Qc by King (2012). Tertiary intrusive bedrock is described as having "numerous fractures" (King, 2012; p. 19), however these are not quantified. Precambrian bedrock is similarly described as having "some fractures" (King, 2012; p. 19).

Similar to those in Saddle, infiltration rates also vary widely in Martinelli basin. According to King (2012), infiltration rates near the Martinelli well locations (Fig. 10) range from $4.07 * 10^{-5}$ m s^{-1} to $6.71 * 10^{-4}$ m s^{-1}. Near the July 2011 Martinelli snowfield extent north of the wells, infiltration rates were measured at both 3.46- and $9.44 * 10^{-5}$ m

s^{-1}. These measurements are well within range of accommodating the ~10 cm of daily

snowmelt that occurs late in the melt season (Caine, unpublished data).
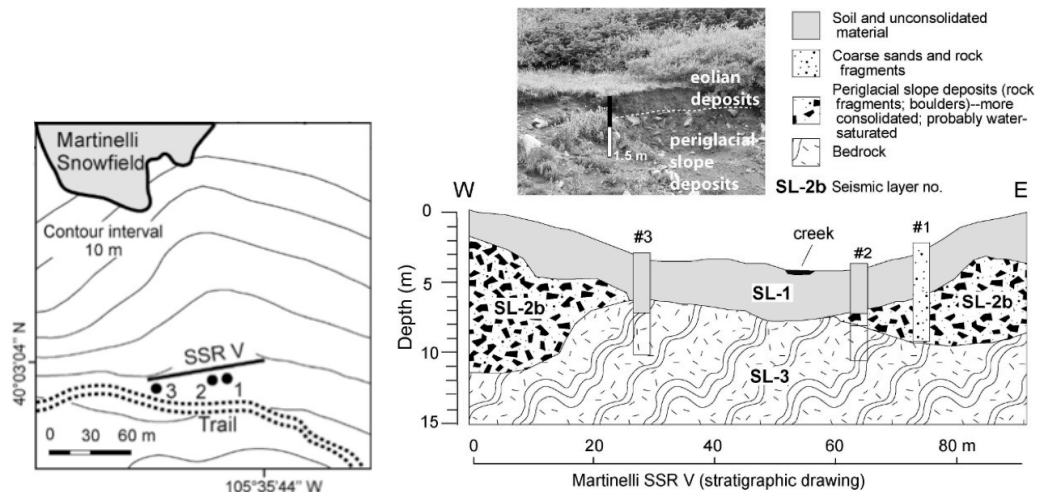
Figure 22. Location (left) and graphical interpretation (right) of Martinelli shallow subsurface refraction (SSR) data. Inset photograph shows a stratigraphic section roughly 40m southeast of the SSR line of eolian deposits overlying periglacial slope deposits (after Leopold et al., 2008).

Hydrograph measurements

Mean daily discharge data from Saddle and Martinelli weirs (Fig. 23) show a

small amount of annual hydrograph peak separation between the two basins. Predictably,

the rising hydrograph limbs of both catchments look relatively similar due to the onset of

the melt season in similarly sized catchments, but Martinelli stream reaches a slightly

higher and broader peak flow than does Saddle, just after the middle of June. The falling

hydrograph limbs differ somewhat because Martinelli stream retains its main water

source later in the season than Saddle, but both rely on the melting of snow and ice as the

source of their discharge.

Diurnal flow patterns are evident in both catchments, especially in the falling limb of the annual hydrograph (Figs. 24, 25). Melt of snow and ice regulate the late-season diurnal pattern in Martinelli stream almost exclusively. This is due in large part to the fact that there is almost no ET in the catchment.
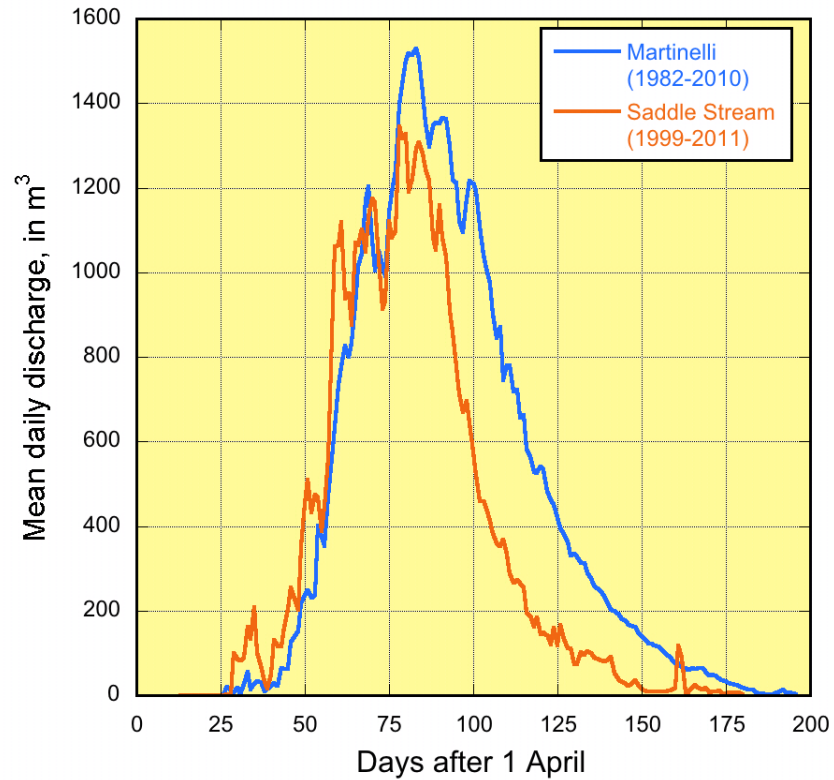
Figure 23. Mean daily discharge in Saddle and Martinelli catchments for the duration of record indicated. On average, peak flow occurs on 15 June and 21 June for each catchment respectively (Caine, unpublished).
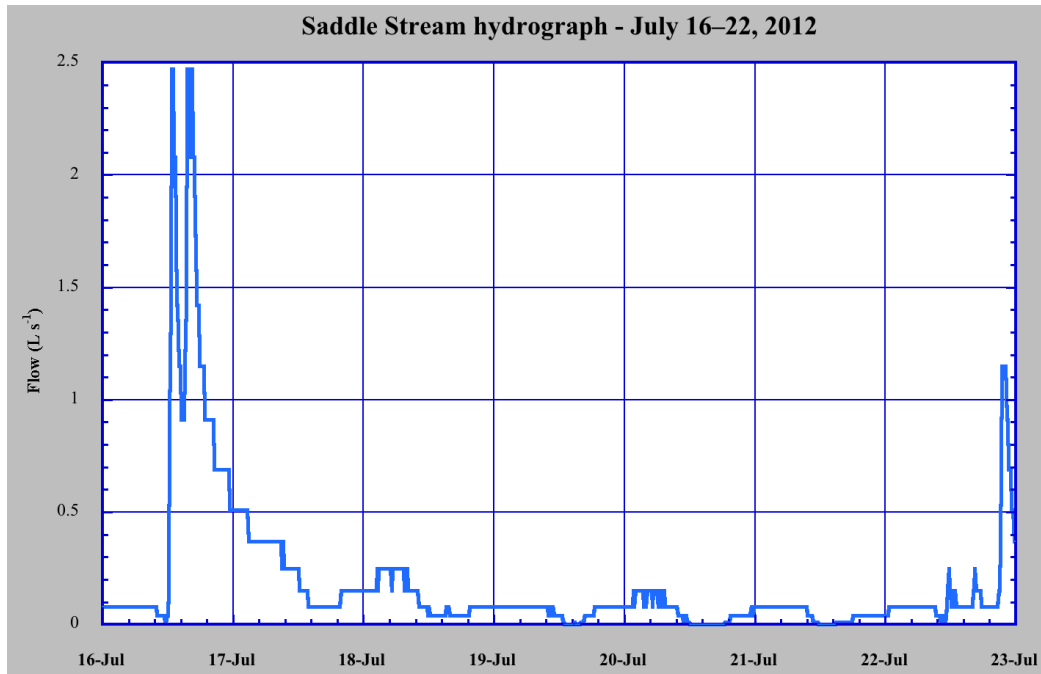
Figure 24. Saddle stream hydrograph showing response to a rain event and weak diurnal periodicity (likely caused by ET, rather than snowmelt as described by Caine, 1992bin Martinelli) during July of 2012. Since 2012 was a low-flow year, and the transducer records at low resolution, the hydrograph shows discrete jumps of 0.4 L s^{-1}.
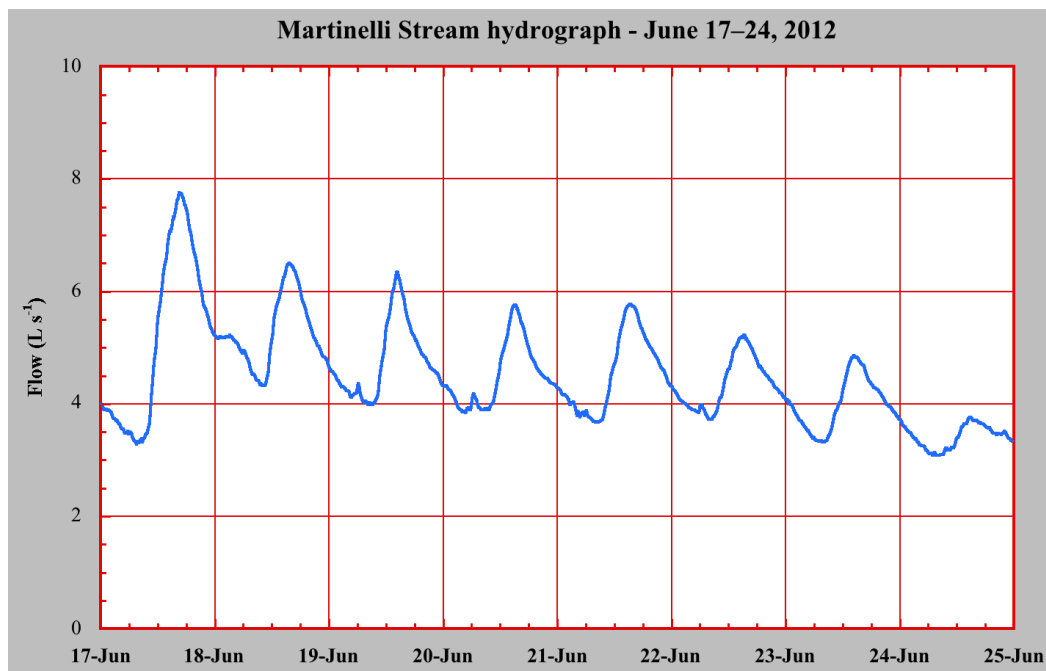
Figure 25. Strong diurnal periodicity exhibited on the falling limb of Martinelli stream in June of 2012 (Caine, unpublished), which corresponds to high groundwater levels.

METHODS

Field methods

My data were provided by field measurements, and by using the ongoing monitoring of discharge in both Martinelli and Saddle streams by the NWTLTER and INSTAAR programs. In addition to using long-term weir data, I measured discharge and water temperature at 17 sites, including the weirs, in Martinelli and Saddle streams two days a week. I measured discharge at ~50-100 m intervals along the channel using a stopwatch and by measuring volume using a heavy duty trash bag placed flush with the bed of the channel. Measurements were taken from the bottom to the top of Saddle catchment on Tuesday and Thursday mornings, and in the Martinelli catchment in the afternoons. Martinelli measurement locations (Fig. 9) were numbered 001-006 (discharge from MS1, a spring below the Martinelli weir, was not included in regular measurements), and Saddle measurement locations were originally named SS1, SS2, and 007-014 from the lowest "Saddle Spring" sites to the top. Measurement site 018 (10 m east of 013) was added later in the field season.

I also measured the area of Martinelli snowfield with a Trimble GeoXT handheld GPS unit running ESRI ArcPad software. T. Nelson Caine provided long-term measurements of snowfield area, discharge at the Martinelli and Saddle weirs, and short-term measurements of rainfall and ablation rate. Caine's data for discharge at Saddle and Martinelli basins are calculated using depth-of flow measurements at each of the weirs.

Discharge

Initially, we took discharge measurements by spanning the stream channel with a Ziploc bag (Fig. 29a), which we used to fill a small trash can, graduated at 10 and 20L volume (Fig. 29b). Measurements were collected in the morning, as often during the field season, the stream ceased to run at the weir in the afternoon (likely because of weak diurnal periodicity caused by ET; Fig. 24). The channels were mostly small enough that the bag could collect most or all of the running water with little escape to the side and little to no backflow (Ziploc bags were too small to be efficient collectors of water, for two reasons: they were not wide enough in some places to cover the whole channel bed, and when they neared full, water would pond behind them). One person held the stopwatch while the other held the bag and filled the trash can. The highest estimated measurement error was 20% (Appendix A).

Figure 26a. Using a heavy duty trash bag to measure discharge in a stream channel in Saddle stream and b. consolidating collected discharge into a graduated bucket.

After two field days, we abandoned Ziploc bags in favor of using a trash bag, because large trash bags held more water, and the lip of the bag was both wider and

easier to shape to the contours of channels. Once we became comfortable with measuring, it was relatively easy for my field partner and me to estimate the approximate time it would take to collect 10 or 20 liters. If the bucket overfilled, we used a graduated cylinder to incrementally measure and remove 250ml at a time until the water level was back at a graduated mark on the bucket.

While the trash bag method was more effective at collecting surface discharge, repeat measurements demonstrated that the Ziploc method achieved 90-95% precision in surface water collection. We tested the precision frequently by measuring flow at the same location three times in a row, or by stopping collection at both 10L and 20L and comparing the 10L fill times.

At several sites, I observed a small amount of flow bypassing our sampler and escaping downstream, but my estimates of this loss were consistently less than 10% of total observed flow in the channel. Loss estimates were made visually, based on the amount of bypass I observed while taking each measurement. Most locations were visually assessed to lose <5% on any given day. Estimated bypass was noted in the field and incorporated into each discharge value. Discharge measurements were most accurate at locations where the channel was relatively well defined (Figs. 27a & b) and least accurate at locations where it was difficult to contain the flow or direct it to a single point (Figs. 28a & b). Unfortunately, although discharge at the Saddle weir was easily measured at the v-notch, a small amount of flow was also escaping beneath the wooden structure. These losses were more significant when flow through the v-notch was low (0.2L/s) or zero.
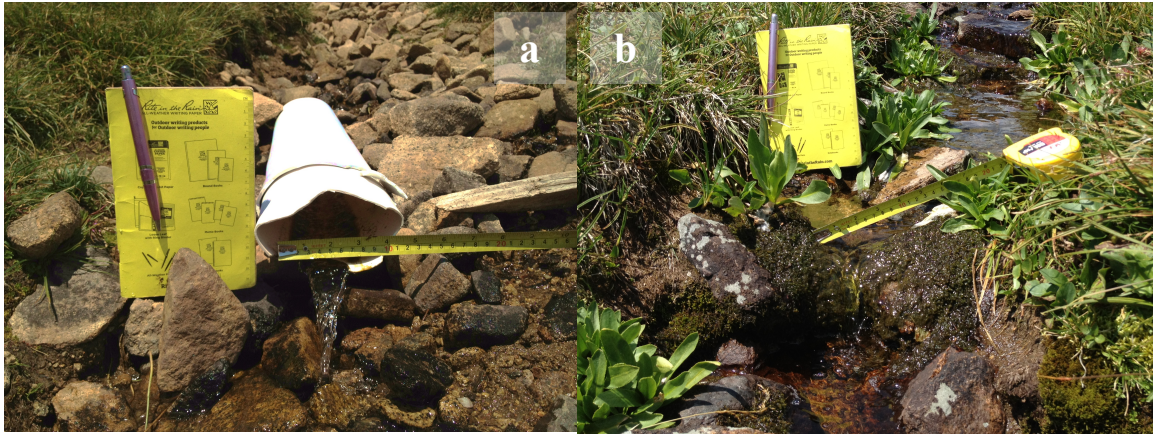
Figure 27a. Closeup of location 014, a spring at the top of the Saddle stream. The small amount of discharge that flows from the spring is funneled into this pipe to obtain a more accurate measurement. b. Location 002 in Martinelli basin, where moss cover on rocks creates a natural weir and measuring discharge with a trash bag is nearly lossless.

Figure 28a. Looking upstream (locally northeast) at location 013, situated below the Saddle wetlands. Most discharge flows diffusely over a flat rock, but some escapes the makeshift weir by flowing behind the rock as viewed from this angle. b. Looking upstream (north) at location 001, in the west channel, on the edge of the Martinelli basin area. Flow travels through sandy gravel, which allows a conspicuous amount of water to escape measurement.

Temperature

Temperature was measured at or just above our discharge sampling sites at the same time discharge was measured. Where possible, we chose sites shaded by a channel bank for consistency and limited solar input (Fig. 29). We used an analog thermometer

for the first two days. In the second week of measurement, we used a digital thermometer (H-B Instrument Company VWR Lollipop-type thermometer, accuracy ±0.5ºC) as well as the analog one. The digital thermometer was better calibrated and gave values on average ~1.5ºC warmer than the analog unit from 0°C to 15 °C. After this was determined, we added 1.5ºC to the spreadsheet values of the previous two field days and used only the digital unit.

Figure 29. Measuring water temperature with the analog ("old") thermometer at the Saddle weir (location 009).

Snowpack and wetland areas

Snowpack and wetland extent were measured every Tuesday and Thursday from July 10 to August 7 using a GPS-enabled Trimble GeoXT handheld field computer

("Trimble" for short). I slowly traversed the outside edge of the snowpack, with the GPS held above my head for best reception quality, while recording locations at 3 or 5 second intervals (Fig. 30). Traverses were always done around midday.

Downslope wetland area was more difficult to measure than snowpack area due to the ambiguity of the wetland boundary. I walked at the edge of the "wet" material with the Trimble to measure the wetland area. I estimated the edge of the wetland by whether or not the material underfoot would hold my weight when stepped on. Often "damp" colluvium would be sufficient to hold my weight without giving, but my boots would sink into "wet" material because material was saturated enough to allow silt to flow laterally when stepped on. Back at the field station, I converted these snow and wetland polyline features in ESRI ArcGIS to polygons to represent each day's extent. I used the Trace Tool in ArcGIS feature creation to allow for faster transfer and exact copy of GPS points.

Figure 30. Measuring snowpack area by traversing the edge of Martinelli snowfield with a GPS.

Collection of streambed location and classification of stream order

I traversed all channels in both Martinelli and Saddle basins using the Trimble to map and classify the order of tributaries. Streambeds, including seasonally dry tributaries, were walked while the Trimble was held overhead. Streams were then field-classified based on estimated Strahler (1957) stream order. Streams that were running directly from springs at the time of recording were given a classification of "1." Channels that were not running but clearly held water at some points in the melt season were classified as order "0." This classification is likely wrong at higher flows, based on observations of large cobble- and boulder-sized clasts in dry streambeds in the field and the fact that some smaller tributaries completely dried up during the field season, and therefore is probably inappropriate or misleading for describing stream order. A more useful descriptor of streams in these basins is a calculation of the approximate flow level or groundwater elevation at which they become dry during the latter part of the melt season, which is shown in my results. Another useful calculation is channel classification of the LiDAR base using RiverTools (Martinelli: Fig. 13; Saddle: Fig. 14).

Analysis methods

Basins

All spatial data were processed in ESRI ArcGIS 10.1 Desktop. We used a 1-meter resolution digital elevation model (DEM) derived from LiDAR point cloud data, provided by the Boulder Creek CZO (Anderson et al., 2012). Basin area was calculated

using Watershed and associated tools (Flow Direction and Flow accumulation) in ArcGIS 10.1, then converted to polygon shapefiles using the Raster to Polygon conversion tool. GPS points taken at measurement locations served as the incipient pour points. If the GPS measurement location did not fall in a map position near enough to the main channel to serve as a satisfactory pour point, and added additional pour points nearer to the DEM channel location and used them in my calculation.

Sub-basins (basin area above discharge measurement points)

To quantitatively compare flow past the measurement points, I needed to calculate the apparent contributing surface area of the basin for each discharge measurement point, based on LiDAR surface topography. To do so, I used GIS locations for each measurement point as pour points, and added adjacent pour points for two meters in each direction perpendicular to stream flow. This prevented "leaks" from bypassing the measurement locations. Then I converted the resulting rasters to polygons and calculated the areas in their respective attribute tables. I then compared these values to the total basin size at each weir.

Short-term hydrologic yield

Short-term hydrologic yield for a significant precipitation event is useful because it removes two important possible summer escape routes for water: E and ET. Since radiation is typically low due to cloudcover, and short-term ET is likely to be < 5 mm d^{-1}, I can approximate E and ET as ~0, leaving only a few remaining variables as I account for the water losses from the basin.

Fortunately for this study, a significant (~100 mm) rain event occurred on July 5–
10, 2012. The event took place in several bursts, the main ones occurring on July 6th,
when 76 mm of precipitation fell in a 24 hour period (N. Caine, unpublished data). I used
this event to study both the short-term hydrologic yield and the flash responses of the
basins.

Two-component mixing model

Two-component mixing models are used to estimate unknown values in otherwise
constrained systems. When two liquids are well mixed, the resulting liquid has the
qualities of both contributing bodies. In this case, the two bodies of liquid are
groundwater and surface water. The temperature and volume of surface water can be
measured quite accurately using the methods described in this study. If water is added to
a channel over a short distance with limited solar heating, and the water properties both
above and below where the addition is made are constrained, I can apply a simple mixing
model to estimate the temperature of the water being added over the reach. If the
discharge increases over distance, the discharge at the upper measurement point can be
subtracted from that of the lower point to get the amount added. Since I measure in
temperature, it is easiest to use temperature values, rather than calories, to make this
calculation.

Once these five values—temperature of the upstream and downstream points and
discharge of the upstream and downstream points plus the contribution from
groundwater—are known, the temperature of the added body (groundwater) can be
estimated using Equation 3:

$$T_z = \frac{T_b * Q_b - T_a * Q_a}{Q_z}$$
[Eqn. 3]

where Q is discharge, T is temperature, $_a$ indicates unmixed, upstream values, $_b$ indicates mixed, downstream values, and $_z$ indicates the properties of the groundwater being added.

Modeling underflow or escape using short-term hydrologic yield

     If I know the amount of precipitation that fell on the basin over a certain time period, and also the amount of water that flowed out of the basin in that time period, I can estimate the amount of water that "should" go by the gage in that time period. If these values do not add up to the amount of input, I can assume that flow leaves the basin by another pathway.

     Groundwater elevation and flow increase after precipitation events. Given Darcy's law, flow increase in the subsurface is not linear given some increase in water table elevation. In a similar manner to the methods of determining short-term yield, if I assume that water table elevation is a proxy for discharge, I can estimate that all of the discharge in the period it takes for water table elevation to return to pre-storm levels is storm-related discharge. During the time it takes for groundwater to return to pre-storm levels, water from the storm is discharging from the basin both as surface and subsurface flow. Once I estimate the return time to pre-storm groundwater depth, I can calculate an underflow value for the basin, given precipitation and discharge for that time period. I call this underflow over time "specific underflow yield." I then subtract estimates for precipitation and ET during the period.

     This calculation is represented in the following equation:

$$\frac{(P_{tot} - Q_{tot}) * A_{basin}}{T} = U_{avg} \qquad \text{[Eqn. 4]}$$

where U_{avg} is the average daily underflow over the time period, in m^3 d^{-1}, P_{tot} is the total precipitation in millimeters that falls on the basin during the storm, Q_{tot} is the amount of specific discharge in millimeters observed during the time period, A_{basin} is the basin area above the measurement point in hectares, T is the amount of time it takes in days for groundwater depth to return to pre-storm levels after the beginning of the event without the influence of other storms. Once average daily underflow is converted to specific subsurface flow in mm for the entire period T, low and high estimates of E and ET are subtracted to obtain a viable range of specific subsurface flow.

Some assumptions and caveats are associated with the use of this formula. The first is that groundwater must return to pre-storm levels, which allows the assumption that all discharge and groundwater elevation increase over the period T is entirely storm-related. The second is that the calculation works best when rain events after the initial one are minimal. One significant caveat to this model is that it is just a first-order calculation to estimate a range of transmission potential values of subsurface conduits.

RESULTS

One would expect to find that discharge follows a typical increase with increased basin area; however my results indicate that this is not the case in the study areas. Most water budget studies rely partly on the accepted relationship between discharge and contributing basin area, and do not account for situations when these relationships break down. Since contributing basin area increases downstream (Table 2, Fig. 31), it is reasonable to expect discharge to increase downstream as well.

Table 2: Contributing basin area at synoptic measurement points (calculated using ArcGIS 10.1 Fill and Watershed tools and LiDAR base; Anderson et al., 2012).

Stream Channel	Measurement Location (Fig. 9)	Basin Area (km^2)
Martinelli	001	0.013
(West Channel)	006	0.013
(Main Channel)	002	0.005
	003	0.140
	004 weir	0.249
	005	0.249
Saddle	018	0.002
	014	0.017
	013	0.068
	012	0.172
	011	0.179
	010	0.204
	009 weir	0.249
	008	0.251
	007	0.252
	Saddle Spring 1	0.253
	Saddle Spring 2	0.253
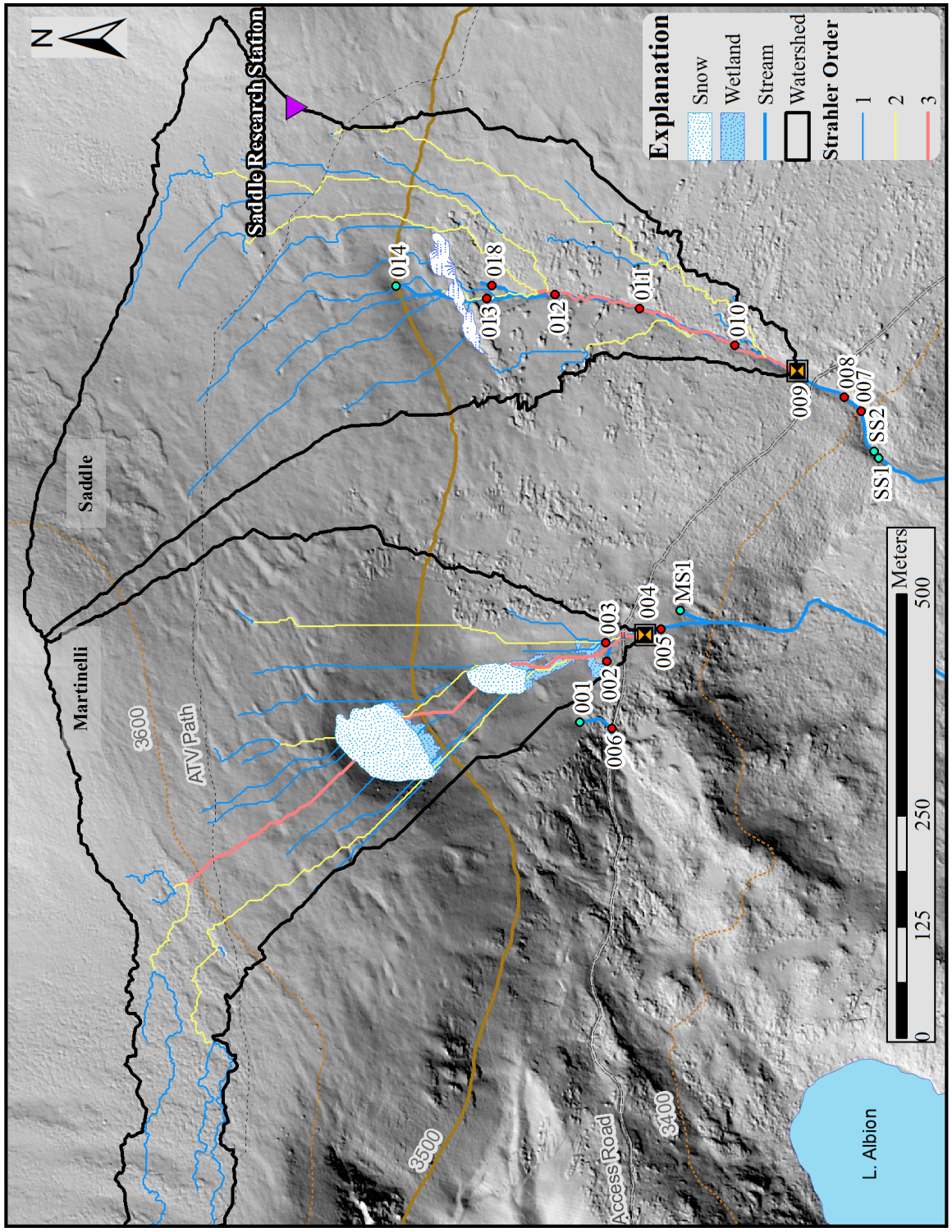
Figure 31 (previous page). Martinelli and Saddle basins, with Strahler (1957) stream order derived from LiDAR base (Anderson et al., 2012).

Results from Saddle basin

Observations

Field observations provided a clue to the processes at work in Saddle. It was clear that something out of ordinary was happening when I observed that flow 100m upstream was more than 0.5 L s^{-1} more than at the weir (ex. Fig. 32). To document the loss at different discharge levels, I collected closely-spaced synoptic measurements (less than 100 m apart) from the emergence point to below the basin outlet.

Figure 32. Flow (~0.5 L s^{-1}) approximately 100 m upstream of the Saddle gage and at the gage (no discharge) at 1:00pm on 8/7/2012.

Synoptic measurements of discharge and temperature

Synoptic measurements show that as contributing basin area in Saddle increases downstream (Table 2), flow in the channel also increases, and then decreases dramatically. Discharge consistently increases over the first 450 meters downstream from the Saddle source (Fig. 33a), and then decreases by more than 50% over less than 100 meters between site 010 and the Saddle weir, site 009.
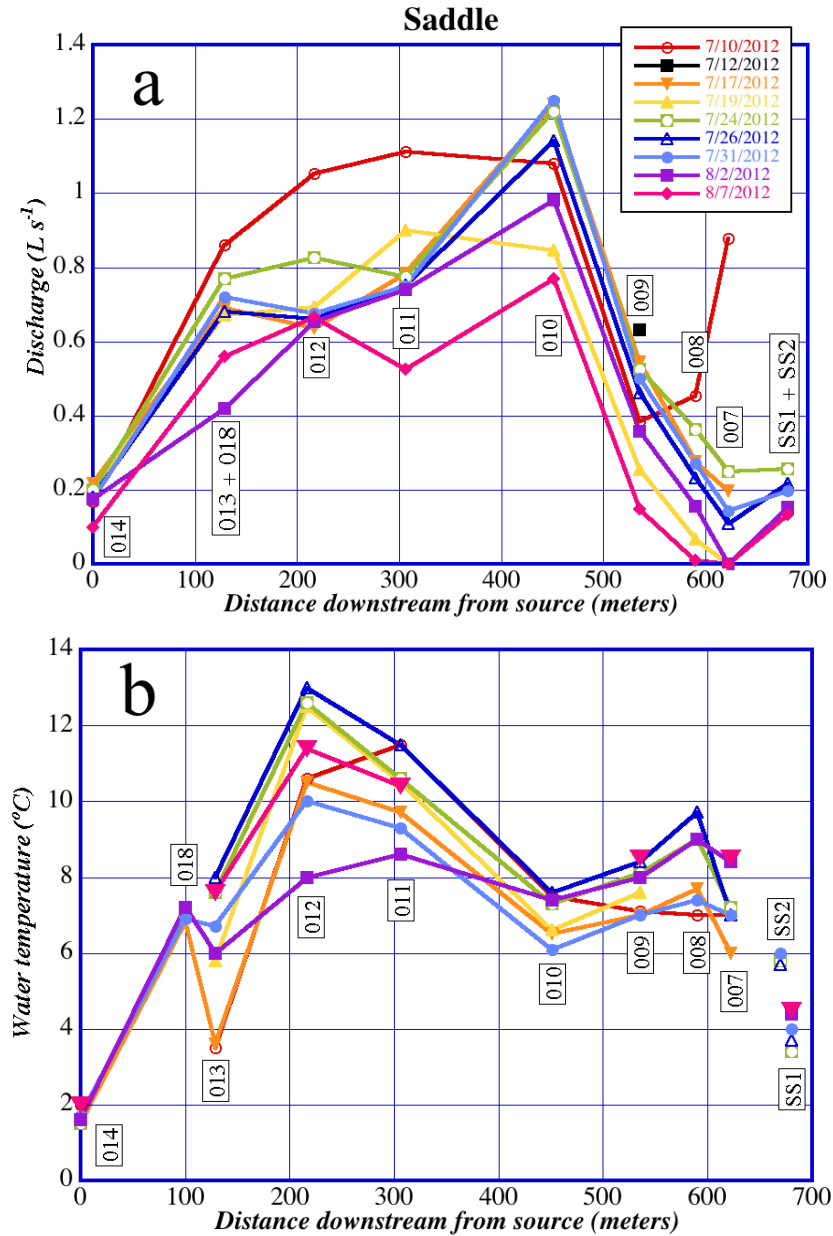
Figure 33a. Saddle stream discharge and b. water temperature, plotted versus distance downstream from source to measurement location.

Temperature values measured in each basin varied widely. Predictably, water temperatures at springs were colder than flow in open channels. For Saddle stream, temperature generally increased for the first 200-300 meters downstream from the source, then decreased reliably to measurement point 010 as flow increases (Fig. 33b).

Snowpack area in Saddle and its relation to measured discharge

The number of area measurement data points of the Saddle snowpack is low ($n =$ 4). The snowpack melts out early on in the spring, and since the snowpack is not visible from the access road, it has not been measured like Martinelli. The average daily yield for these five days in 2010 and 2011 at the Saddle weir exceeds the calculated discharge from the snowpack. Three of the five points were collected before peak discharge in the basin, which suggests that in some years the snowpack disappears completely before peak annual discharge occurs. Because pre-peak discharge does not correlate simply with snowpack area, the relationship between the Saddle snowpack and discharge cannot be used to quantitatively constrain specific yield calculations (Fig. 34).

Saddle catchment - 2010–2011

$y = 8.8e+2 + 0.37x$ $R^2 = 0.38$

Measured flow, in $m^3\ d^{-1}$

Discharge predicted from snowmelt, in $m^3\ d^{-1}$
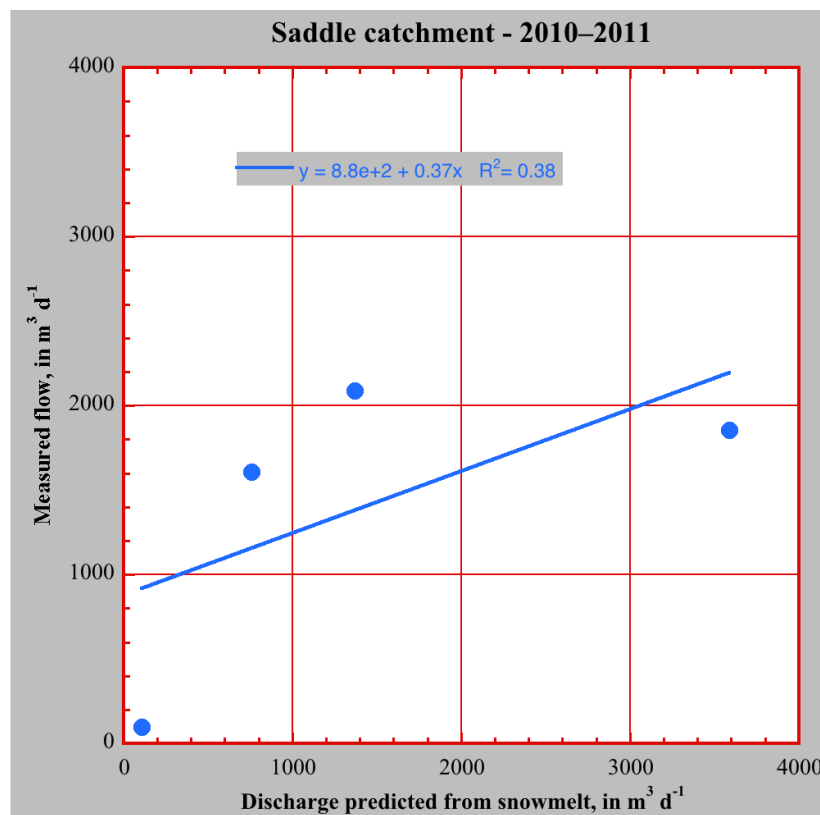
Figure 34. Snowpack area vs. discharge at the Saddle weir, based on 4 measurements during the 2010 and 2011 field seasons.

Correlation between groundwater depth and discharge

When analyzing groundwater depth as an analog to discharge and vice versa, it is helpful to know the correlation between the two values. Post-peak discharge in both Martinelli and Saddle streams was compared with groundwater elevation measurements made by Morgan Zeliff (written communication, 1/7/2013), Jessica King (King, 2012), Rory Cowie (Cowie, 2011), and others (Fig. 35). These values were closely crosschecked to ensure they were indeed post-peak snowmelt discharge, and that there were no anomalous increases at one well and not at the others, that might indicate a subsurface ice lens or other local interruption of flow. Anomalous water table elevation occurred mainly before peak flow and in the days shortly after peak flow.
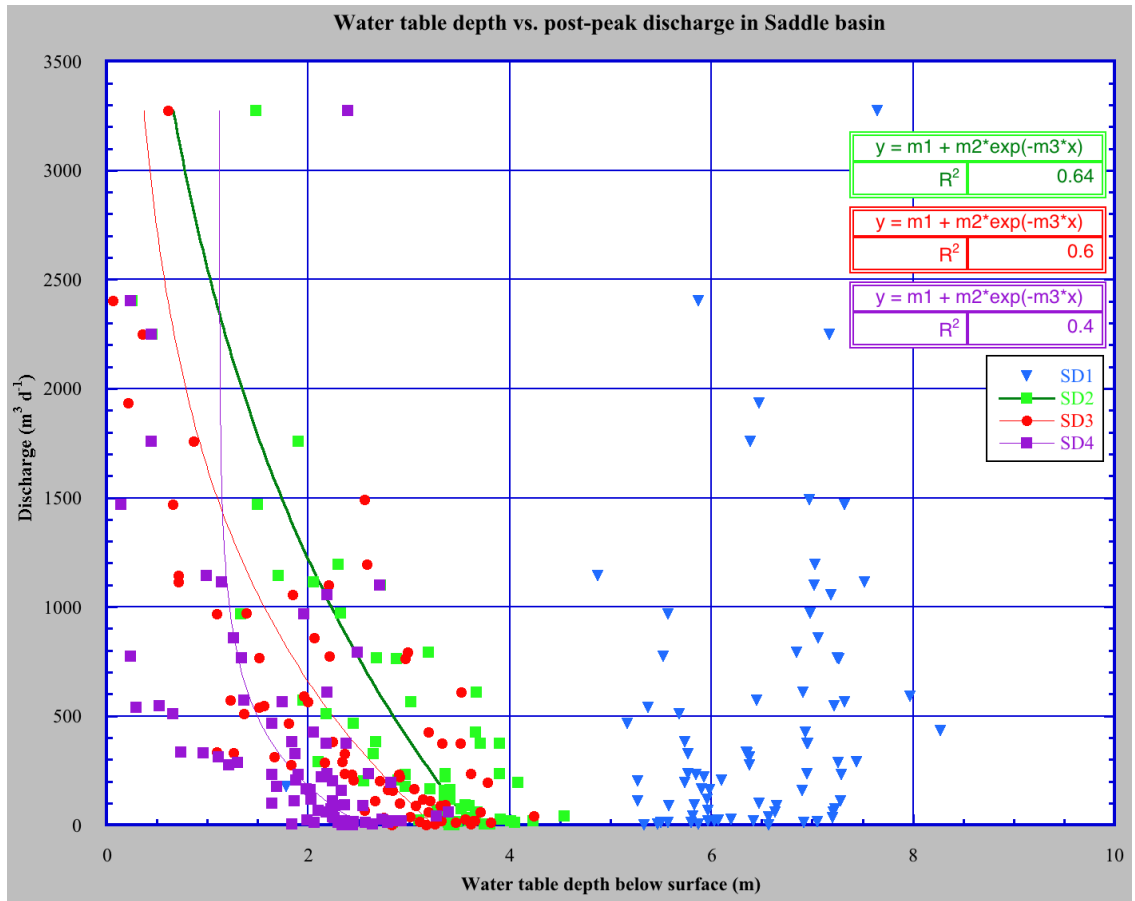
Figure 35. Correlation of Saddle weir discharge (Caine, unpublished) with water table depth (King, 2012). X-axis represents the depth (in m) to groundwater relative to the ground surface. Y-axis plots daily discharge (in $m^3 d^{-1}$). SD1 (blue, no trend) is drilled near the Saddle Tundra Lab Research Station, and appears to be mostly hydrologically disconnected with the rest of the wells and the basin as a whole. SD2 (green), SD3 (red) and SD4 (purple) show much more characteristic groundwater depth correlation with post-peak discharge.

Short-term specific yield

   Specific yield calculations for both Martinelli and Saddle weir locations were quite low. The first synoptic measurement, from July 10th, was 3-5 days after a multi-day ~100 mm rain event. This resulted in water table elevation increase in both basins, and caused significant increase in discharge after the storm (Fig. 36, around 95 days after April 1, 2012). Using the July 10th rain event and the associated spike and recession in discharge, I calculated a short-term specific yield of 2.2% for Martinelli stream and 2.7%

for Saddle, compared to 51.5% for the nearby Green Lake 4 basin (Table 3; Fig. 37).

Since discharge in Saddle was zero for a period of days before the storm, I was able to

assume that all discharge at the weir was storm-related (at least in the first 2-5 days,

before increased water table elevation became the main factor in the amount of surface

discharge). This is significant because short-term events allow us to rule out ET as a

potential cause of low short-term yield values.
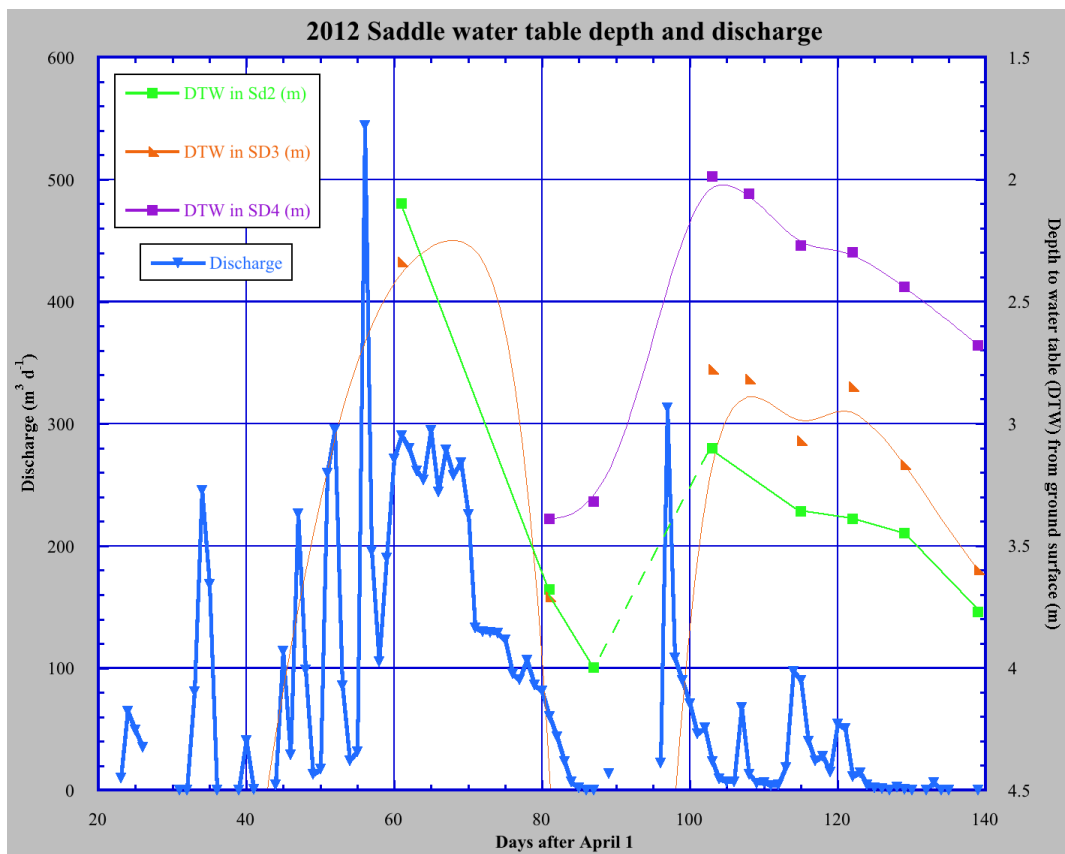
Figure 36. Saddle groundwater depth and discharge over time in the 2012 melt season. Groundwater data have low temporal resolution, but note the estimated later lag-to-peak in the wells compared to discharge at the gage (Zeliff, unpublished data).

Table 3. Calculations of specific yield, using values greater than baseflow for the period of July 5-10, 2012.

Date	University Camp ppt (mm)	Est. GL4 ppt † (mm)	GL4 Q (m^3d^{-1})	Martinelli Q (m^3d^{-1})	Saddle Q (m^3d^{-1})	Calculation
4-Jul-2012	0	*0*	15931	182	0	
5-Jul-2012	7.62	*5.11*	15476	207	22	
6-Jul-2012	78.74	*52.76*	74142	424	313	
7-Jul-2012	12.7	*8.51*	39911	319	108	
8-Jul-2012	17.78	*11.91*	21623	279	90	
9-Jul-2012	0	*0*	17040	215	71	
10-Jul-2012	0	*0*	14915	182	47	
11-Jul-2012	2.54	*1.70*	12446	161	51	
12-Jul-2012	0	*0*	19045	149	13	
Total, 7/05 - 7/10	116.84	*79.98*	183107	1626	651	
			15423	182	0	Baseflow ‡
			90570	534	651	Stormflow (m^3)
			41.19	2.15	2.63	Storm runoff (mm)
			51.49	2.20	2.68	Specific yield (%) §

† GL-4 precip. calculated using linear rainfall-distance function between U.Camp, Albion (98 mm), and GL4 (GL4 ppt. = U. Camp ppt * 0.67)

‡ calculated as average of daily discharge values from before and after storm flow (July 5 and 10), except for Saddle where all discharge was assumed to be storm-related

§ Martinelli and Saddle yield calculated using Albion precipitation for 7/05 - 7/10 (98 mm) as proxy

Precipitation and Runoff by Basin - (July 5–10, 2012)
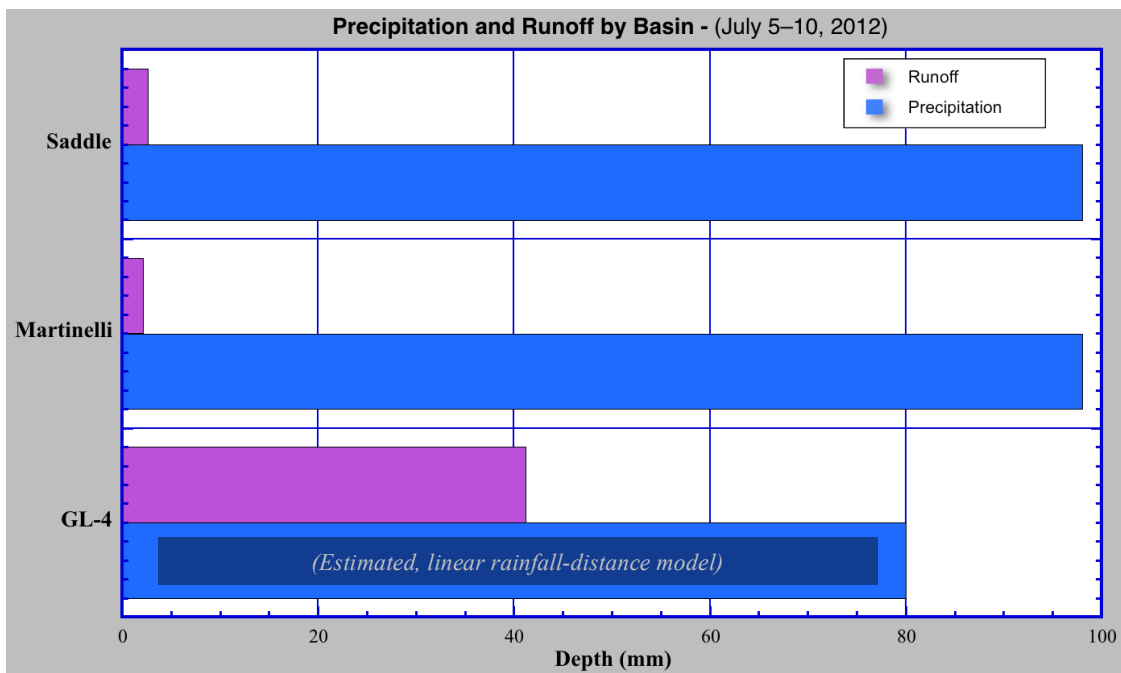
Figure 37. Graphical representation of short-term yield in three basins for the period July 5 through July 10, 2012. Precipitation at Green Lake 4 was estimated using a linear distance

model extrapolating the gradient between precipitation at the National Resources Conservation Service (NRCS) University Camp Meteorological Station (NRCS, 2012) and at the Albion Meteorological Station (Caine, unpublished).

Results from Martinelli basin

Synoptic measurements

Martinelli stream showed a different discharge irregularity (Fig. 38a). Discharge decreased in a linear fashion towards the gage throughout the field season, and the small channel fed by a cold spring (site 001) west of the watershed boundary appeared to direct most of its discharge out of the basin, and water soon disappeared back into the ground. Below the lowest measurement point, near the glacial wall of the U-shaped valley, cold water emerged from a channel on the east side of the main channel in Martinelli (MS1 in Fig. 9) that was measured at 1 liter per second on August 7. Water chemistry results from this location showed that this water showed a similar amount of nitrogen as the water in the main Martinelli channel (C. R. Corona, personal communication, May 10, 2013). This indicates that it likely originates from the Martinelli snowpack, because nitrogen fixation would remove the ion from the water if it passed through a more heavily vegetated area like the stand of white pine between Martinelli and Saddle. Further down the channel, as the slope increased and bedrock exposures could be seen, field observations showed that discharge increased again significantly with no obvious surface source. Temperature was variable down the Martinelli channel as well, but the data were not quite as striking, since the resolution of collection points in Martinelli basin was not as detailed (Fig. 38).
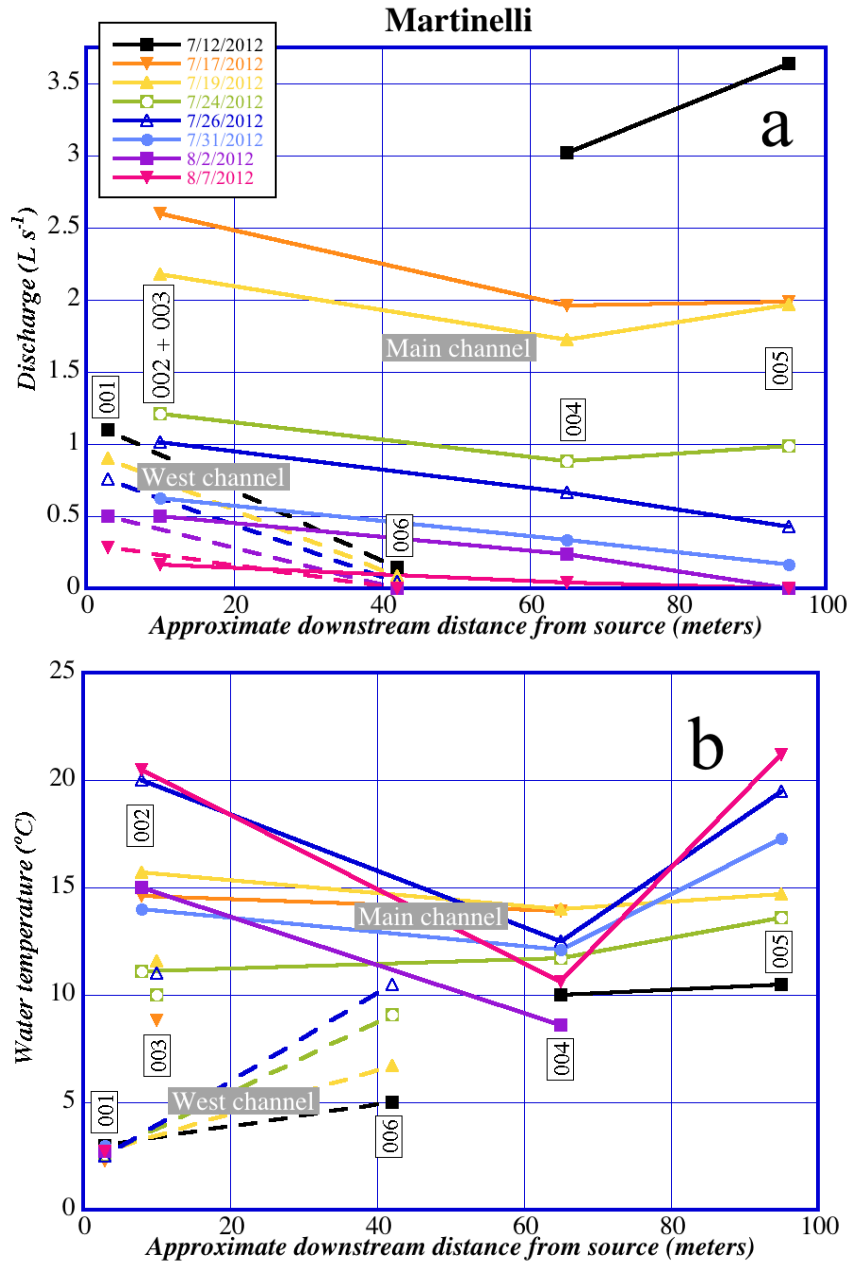
Figure 38a. Martinelli stream discharge and b. water temperature, plotted by channel and organized by date versus distance downstream from emergence point. West channel (Fig. 9) flows out of the calculated basin area.

Snowpack measurements

Snowpack area measurements showed an exponential decrease over the field season (Table 4).

Table 4: Martinelli snowpack area measurements taken using Trimble GeoXT handheld GPS during the 2012 field season.

Date	Snowpack Area (m²)
7/10/12	8466
7/12/12	6855
7/17/12	5244
7/19/12	4234
7/24/12	2600
7/26/12	2043
7/31/12	1084
8/2/12	523
8/7/12	2.0

Correlation between water table elevation and discharge

As was done in Saddle, Martinelli basin groundwater depth was compared with water table depth measurements made by Morgan Zeliff (written communication, 1/7/2013), Jessica King (King, 2012), Rory Cowie (Cowie, 2011), and others (Fig. 39).
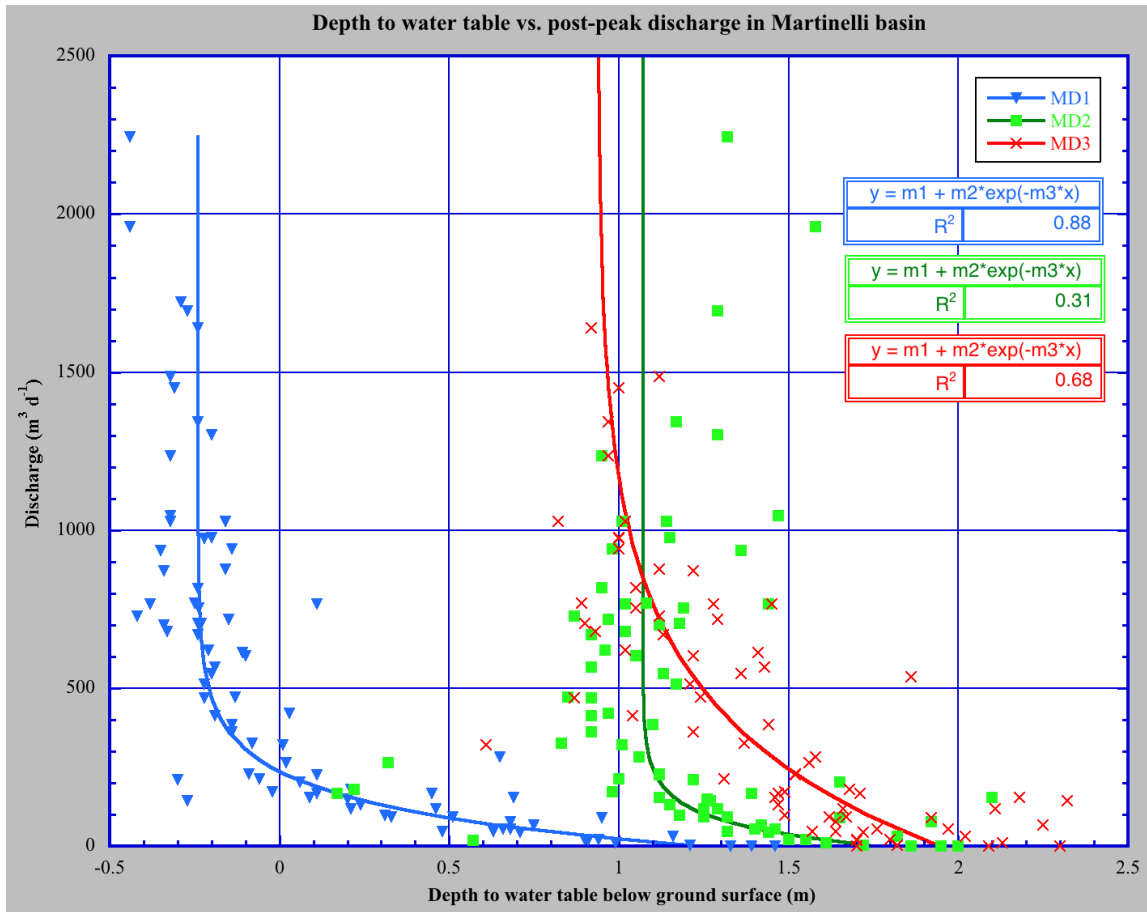
Figure 39. Groundwater depth vs. discharge for Martinelli wells (Fig. 10) over the period 2005-2012. X-axis represents the depth (in m) of the groundwater table below the ground surface. Y-axis represents post-hydrograph peak discharge (in m^3d^{-1}). MD1 (3426.1 m) shows the best correlation, MD2 (3426.7 m) and MD3 (3429.0 m) show less correlation.

DISCUSSION

Fundamental to the study of surface water hydrology is the idea that catchments are watertight and that discharge characteristically increases downstream as basin area increases. Flow in the study areas does not follow this pattern (Table 2; Figs. 33a, 38a). Discharge in Saddle basin decreases sharply over less than 100 meters of channel distance. In Saddle, evaporative processes cannot cause the decrease in discharge between the two locations because it occurs over such a short interval. In Martinelli, it is clear that water loss is occurring because snowpack area, density, and melt rate measurements predict significantly more flow than is measured at the weir. Therefore, as discussed below, water loss in both basins must be caused by flow into more favorable hydrologic pathways, resulting in underflow past the gage.

Testing accuracy of hand-drawn snowpack area with GPS-measured snowpack area in Martinelli basin

Dr. T. Nelson Caine has calculated air-photo based Martinelli summer snowpack area from field sketches made each year since 1991. Dr. Caine sketches the area of the snowpack in relation to accurately placed landmarks on a snow-off photograph. Caine's values were correlated with GPS measurements of snowpack area in the 2010, 2011, and 2012 field seasons (Fig. 40), generating a conversion factor (0.914) that was applied to all area values in the 21-year snowpack area dataset. The correlation is excellent thanks to the precision and care with which Caine has made these measurements, and the offset likely reflects rectification errors in the photograph.
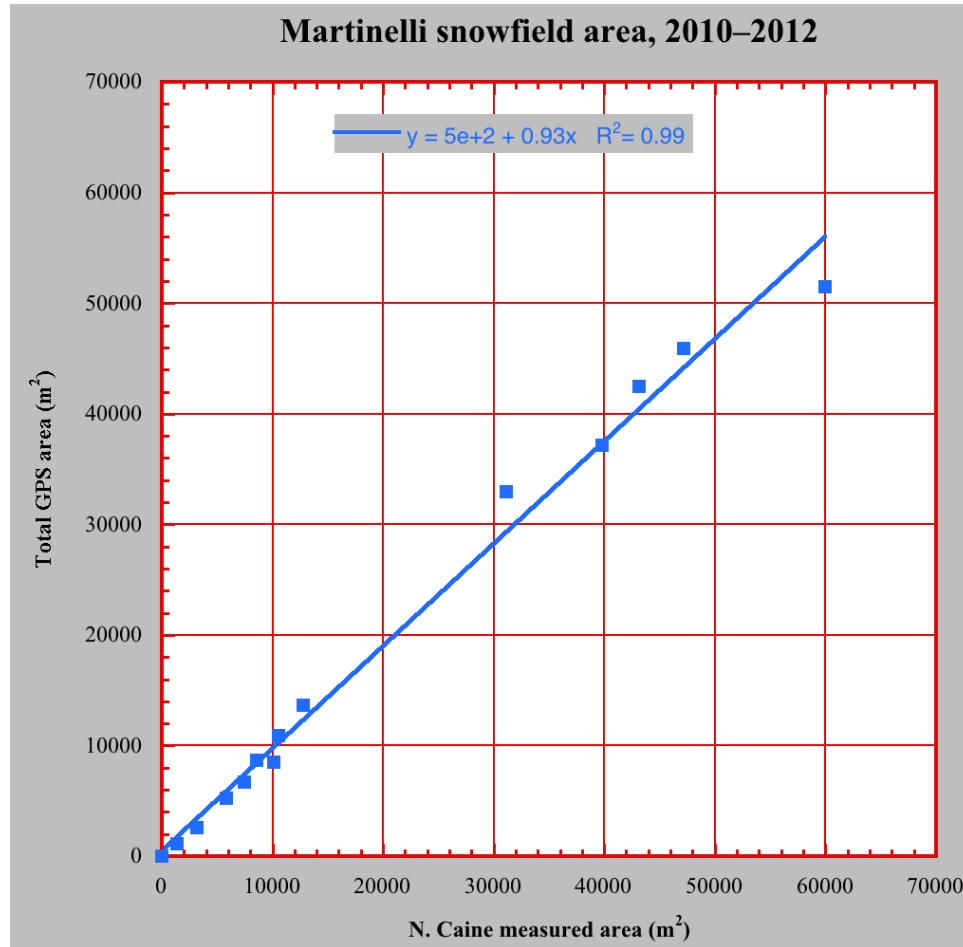
Figure 40. Correlation of sketched Martinelli snowpack area with GPS area for 18 field days in the years 2010-2012. Note high R^2 value.

Short-term hydrologic yield

   Short-term specific yield calculations (Table 3; Fig. 37) are well constrained in

Saddle basin due to the fact that no discharge was recorded at the weir before the storm,

so we can for the moment assume baseflow is zero and subsequent recorded discharge for

a period of a few days is entirely comprised of runoff from storm precipitation. In the

short term, some precipitation that falls on the basin is used to recharge groundwater. The

hydrographs of both basins show several distinct peaks (Fig. 41), as if shallow, rapid flow

was dominant during that period, yet both basins still discharged less than 3% of the

precipitation that fell on them. This result supports annual hydrologic yield measurements

and creates more confidence in the statement that the basins lose water due to underflow.
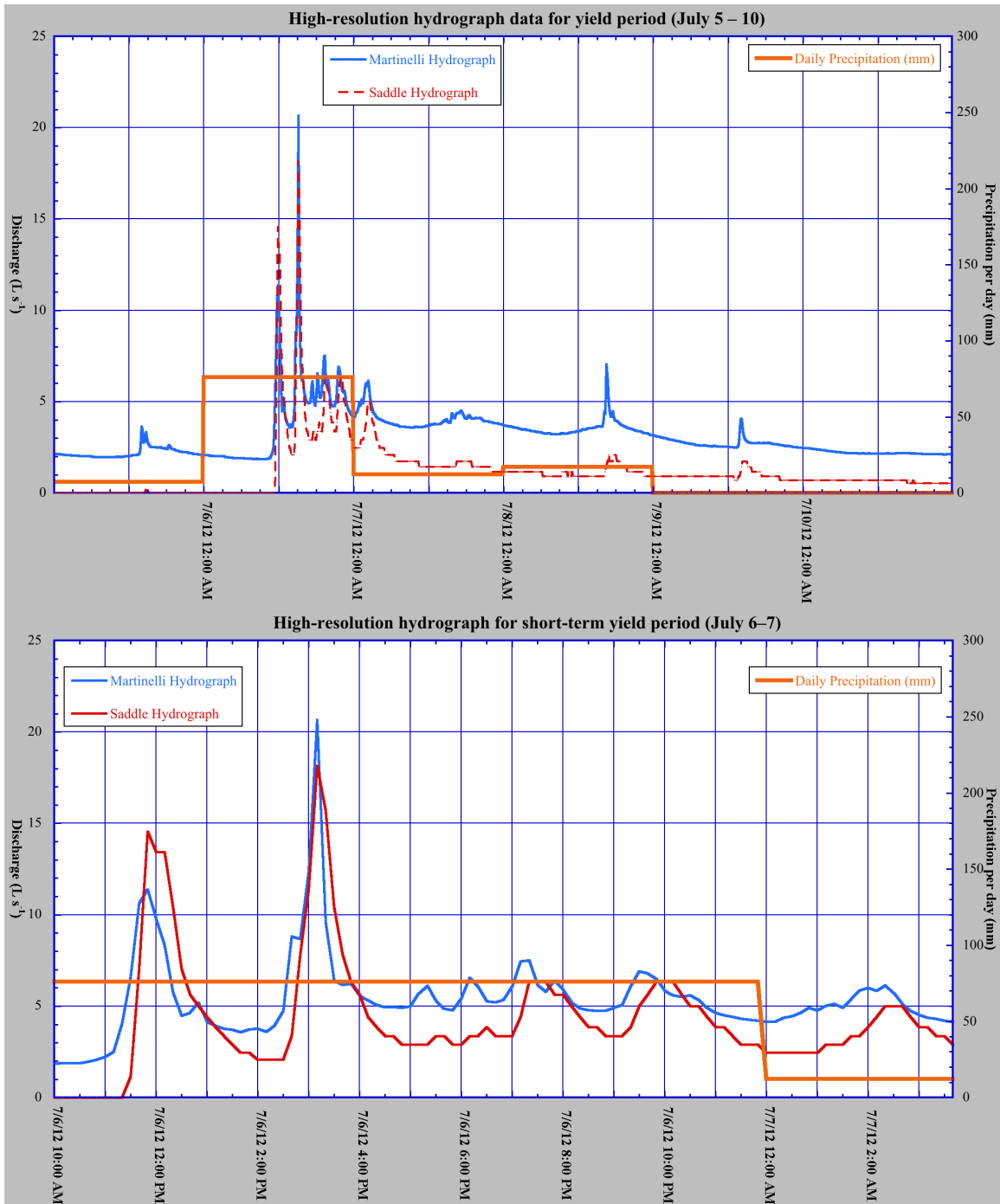
Figure 41a. Martinelli vs. Saddle discharge, represented by 10-minute hydrograph data during the July 5-10 rain event used in the short-term yield calculation. The basins' peak discharge for this time period is in the same 10-minute time segment, however closer inspection of b. high-resolution data reveals a slight lag from Martinelli to Saddle for several smaller hydrograph peaks during the July 5–10 rain event. Martinelli hydrograph

remained higher than Saddle as flow decreased, likely because it was sustained by snowmelt recharge. Diurnal snowmelt signature in Martinelli is mostly lost, likely because it is drowned out by afternoon rainstorms in the days following July 6.

Hydrologic responses

Because the Saddle stream does not have a lasting contribution from snowpack (and therefore its groundwater height does not remain elevated), its baseflow level is lower than that of Martinelli's. Martinelli wells show relatively little change in groundwater depth after significant precipitation (Fig. 42) as compared to Saddle wells (Fig. 36), which show a more typical groundwater elevation increase in response to precipitation. This could result mean that Martinelli has greater permeability and thus is able to accommodate more groundwater flow. Martinelli and Saddle surface discharges have a nearly identical response to rainfall, however when precipitation rates are high, Martinelli's lag to peak is slightly shorter on average than Saddle's (Fig. 40b). The reason for this is unclear, but could be caused by greater wetland storage in Saddle. Further hydrograph analysis of intense storms may give clues.
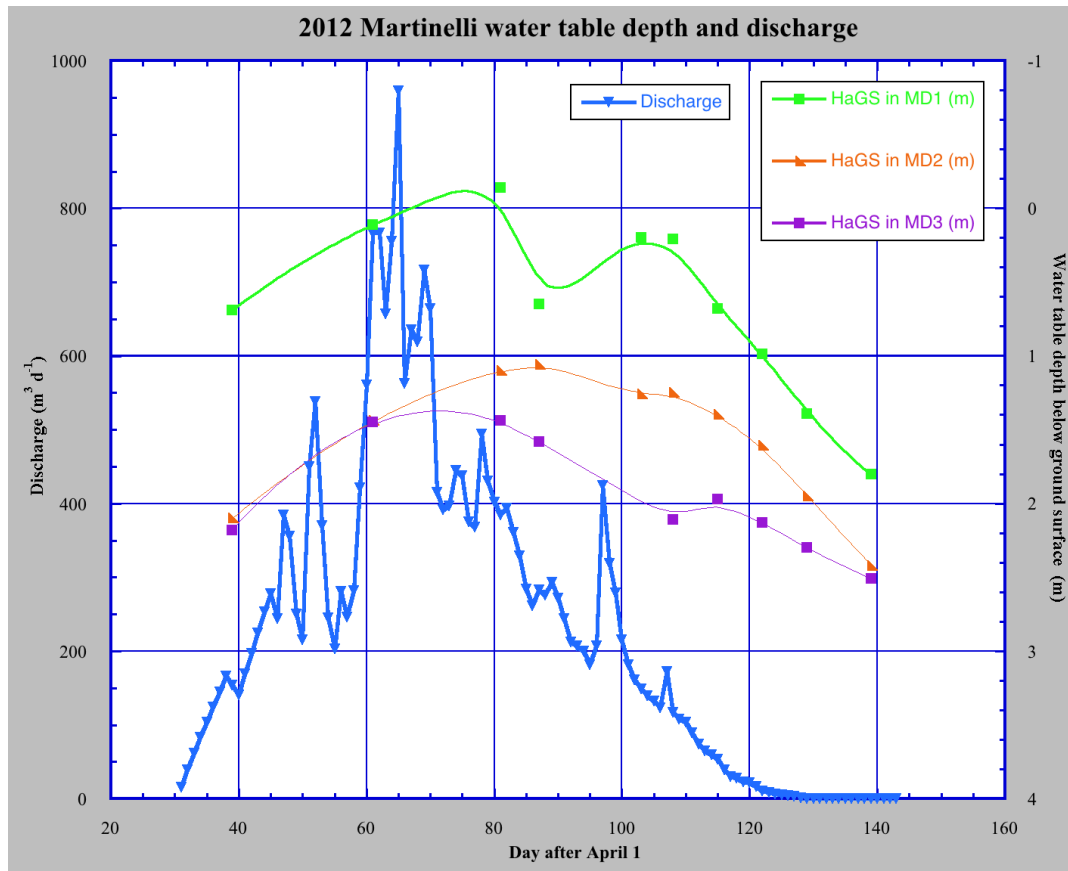
Figure 42. Martinelli water table depth and discharge over time in the 2012 melt season. Note the hydrologic response to the 100 mm rainfall event between days 95 and 100—the July 5 event used in the specific yield calculation (Table 3).

Saddle basin

Since the Saddle stream is not as accessible as Martinelli for snowpack measurements, it has only been measured by GPS a few times in the years 2010 and 2011. Saddle snowpack does not likely last very long past peak discharge, but collecting more measurements would greatly aid the analysis of the basin. I plot all of the current data points in my results in order to show the need for more measurements (Fig. 34). Despite this dearth of data, it is still possible to calculate the loss of water to underflow in Saddle basin and how it relates to the water budget using other methods.

Application of synoptic discharge to water loss

Results of synoptic measurements in Saddle stream indicate a loss of surface discharge to underflow (Fig. 33a). Since loss between the two points has an approximately linear relationship based on discharge (Fig. 44), I extrapolated the trend to predict discharge at location 010 when measured flow at the gage (location 009) is zero. From the average amount of discharge lost from channel (0.66 L s^{-1}, shown in Fig. 43) I calculated an approximate minimum discharge volume lost daily in Saddle stream (50 m^3 d^{-1}), by extrapolating the loss of mid-afternoon discharge above the gage out to the whole day. This is the best-constrained method of estimating low-flow losses in the basin. These are minimum limiting values for channel losses, since I will show that the flow through subsurface conduits can also be estimated using other techniques. We will then see that the value discussed above is likely an underestimate.
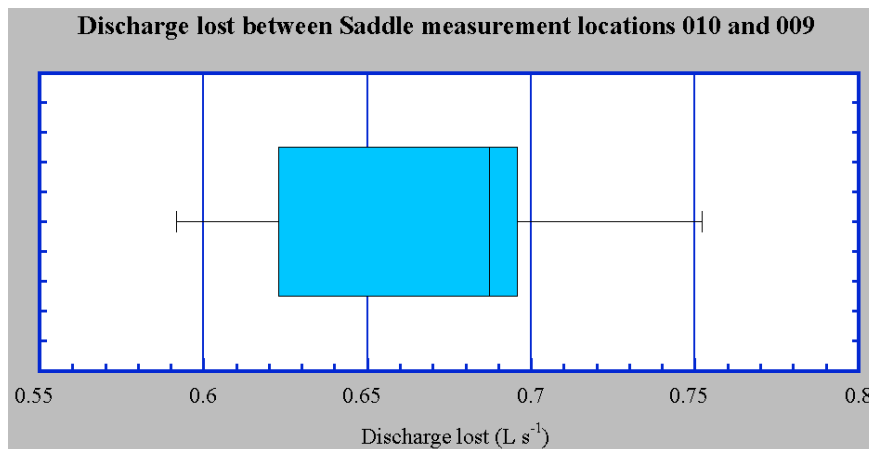
Figure 43. Box plot of discharge lost between Saddle measurement locations 010 and 009. Mean value is 0.67 L s^{-1}.
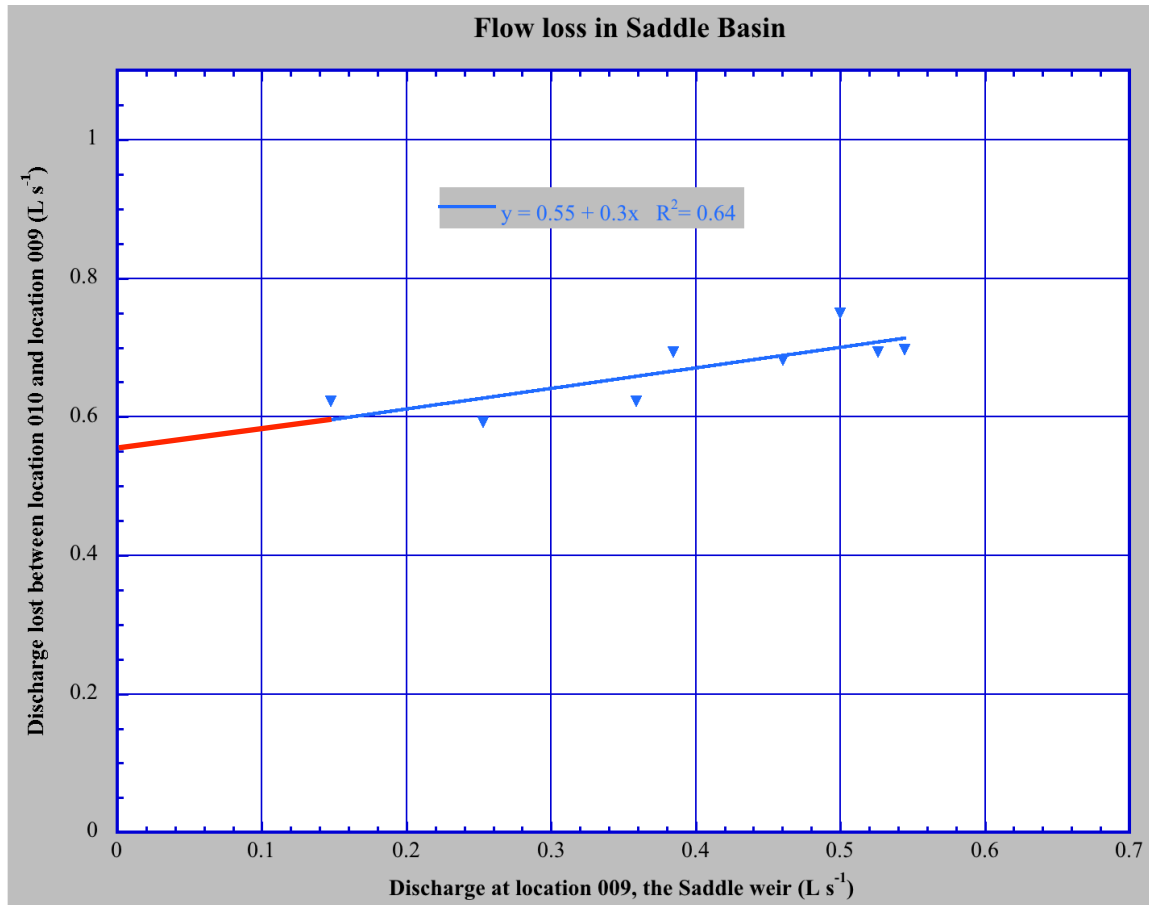
Figure 44. Comparison of discharge using measurements at location 009 (X-axis) and flow lost between locations 010 and 009 (Y-axis), with best-fit line (blue). Extrapolation (red) shows that location 009 (the Saddle weir) ceases to discharge when location 010 is discharging less than about 0.55 L s^{-1}. This relationship shows an increase in groundwater transmission at higher head, consistent with Darcy's law (1856).

Synoptic measurements and mixing model

Water temperature changes nearly as dramatically over distance as does discharge in Saddle. Summer stream water temperature, like discharge, typically increases asymptotically downstream as it gains energy from sensible heat and solar radiation. In Saddle, the results show that temperature reaches a peak near 200 m downstream from the source (Fig. 33; location 012), but rapidly becomes colder again as discharge increases downstream. However, discharge increases in the absence of any surface

tributary, so we must assume that groundwater admixes with surface water, possibly in a discrete hyporheic zone. Discharge increases from location 011 to a peak at point 010. Since temperature decreases over that period significantly, we can assume that a colder body of water is added to decrease the stream temperature. I used the simple mixing model described in Eqn. 3 order to determine the temperature of groundwater being added (Table 5).

Table 5: Inputs and outputs (far right, grey) of simple mixing model described in Eqn. 3. Discharge (Q) is in Ls⁻¹ and temperature (T) is in ºC.

Date	Starting Q (loc. 011)	Starting T (loc. 011)	Ending Q (loc. 010)	Ending T (loc. 010)	Added Q (GW)	Added T (GW)
7/17/12	0.78	9.7	1.24	6.5	0.46	1.00
7/24/12	0.77	10.6	1.22	7.3	0.45	1.65
7/26/12	0.75	11.5	1.14	7.6	0.39	0.10
7/31/12	0.75	9.3	1.25	6.1	0.5	1.30
8/2/12	0.74	8.6	0.98	7.4	0.24	3.70
8/7/12	0.53	10.4	0.77	9	0.24	5.91
Mean:	0.72	10.2	1.10	7.32	0.38	2.28

Because Saddle groundwater has not traveled very far, its temperature speaks volumes about the properties of the material it travels through. Calculated groundwater temperature increased throughout the field season as calculated in Table 5 and as measured in synoptic measurements (Table 6), which could mean that the temperature was partially regulated by melting ice lenses further upbasin. Although they found no ice lens in the subsurface just above Saddle, Lewis et al. (2012) and C. R. Corona (unpublished) did measure several cold seeps that indicated the presence of ice at higher elevation (Fig. 45). Lewis et al. (2012) also present a temperature–depth model for the

subsurface at a given mean annual temperature. This model may preclude the presence of

permafrost, but does not rule out ice lenses at different depths at this time of year.

Table 6: Measured groundwater temperatures over time (in ºC) on Niwot Ridge, July-August, 2012

Date	Saddle Location 014	Martinelli Location 001
7/10/12	1.5	2
7/17/12	1.5	2.3
7/19/12	1.6	2.7
7/24/12	1.5	2.6
7/26/12	1.6	2.5
7/31/12	1.7	3
8/2/12	1.6	2.7
8/7/12	2	2.7
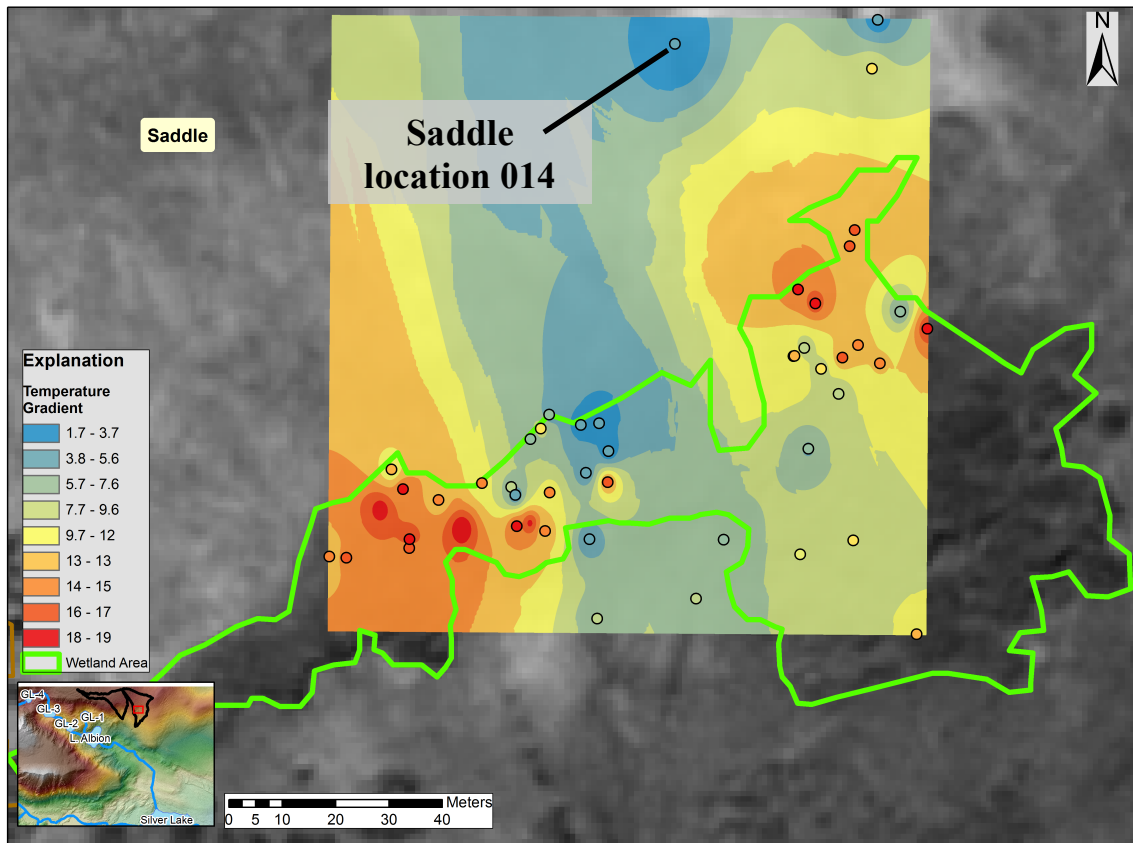
Figure 45: Inverse distance weighted (IDW) interpolation model of measured temperatures in and around the Saddle wetland area on 7/31/12, showing Saddle location 014. Model shows colder temperatures in the center of the wetland and warmer temperatures towards

the edges. Such cold temperatures at the springs could indicate the presence of upslope ice lenses.

Since we know the temperature of two other groundwater sources in Saddle (Table 6), the temperatures derived from the mixing model make sense, and indicate that the groundwater, even at low flow, has a unique signature. The model also serves to support the hypothesis that the water added over this stretch is indeed from a discrete groundwater source.

Estimation of carrying capacity of subsurface conduits using short-term hydrologic yield (modeling underflow volume)

Since we know groundwater depth in the upper reaches of Saddle basin, I can estimate the amount of time it takes for the groundwater levels to return to pre-storm levels. The July 5-10 storm began 96 days after April 1, so I assume that groundwater recharge began on that date. Although no groundwater measurements were taken after October 1, given the trend in groundwater elevation measured in Saddle (Fig. 36), it seems reasonable to assume that groundwater returned to pre-storm levels approximately 50 days after the storm. In other years, an order of magnitude smaller precipitation event (like the ~10 mm one shown in the 2009 Saddle hydrograph; Fig. 16) has resulted in an approximately 5-day return to pre-storm groundwater levels. Since there is no way to remove the effects of groundwater elevation increase due to subsequent storms, we must include the inflow caused by subsequent storms in the inputs to the model as well.

Table 7: Inputs and outputs of the subsurface carrying capacity model in Saddle stream.

Variable	Value	Unit

P_{tot}	218	mm
Q_{tot}	51.6	mm
A_{basin}	250	ha
T	50	days
U_{avg}	832	$m^3 \, d^{-1}$

When this model is applied to the July 5 rain event and the 50-days following in Saddle stream, the results indicate that on average, between than 800 $m^3 \, d^{-1}$ of water discharges from the basin each day, at an average rate of about 9.63 L s^{-1} (Table 7). That equates to about 167 mm of specific groundwater flow.

E and ET are values estimated for the melt season, so since the melt season lasts 120 days on average in Saddle, and $T = 50$ days, we can approximate that 40% of E (89 mm) and ET (104 mm) occur in this period. However, subtracting both of these values from specific groundwater flow gives -27 mm of estimated specific groundwater flow, which obviously cannot be true. Since approximately 50 $m^3 \, d^{-1}$ (or ~10 mm of specific discharge over time T) of low-flow surface discharge become groundwater flow between locations 010 and 009, and that value is likely higher at higher flows, it is reasonable to hypothesize that this should be the lower bound of underflow in the basin. Therefore, I can estimate that between 10 and 167 mm of specific discharge is lost over time T. If I extrapolate this value to the entire melt season, I get that anywhere from 25 to 417 mm of specific underflow occurs in Saddle basin.

If the higher end of the estimate is true, as is likely for Martinelli (discussed below), this finding is substantial, and the implications for this volume of water underflowing the gage are significant; not only for estimates of E and ET, but for interpretations of the surficial geology of the basin as well.

Martinelli basin

Long-term post-peak yield

I examined the relationship between discharge predicted from snowmelt (and daily rainfall) in Martinelli basin and flow recorded daily at the gage. I used the regression to predict the amount of snowmelt that escapes the gage based on how much snowmelt there is per day in Martinelli basin. This is a minimum estimate for how much water escapes the Martinelli gage.

On average, the Martinelli snowpack ablates 0.1 m per day, and during the post-peak discharge period the snowpack has an average density (ρ) of 0.5 g cm^{-3} (Caine, personal communication; modified from Gutmann et al., 2012). Using these values and weekly snowpack area measurements from the years 1991-2012 (Caine, unpublished data), I estimated meltwater volume for each field measurement day in cubic meters. I then compared corresponding days' discharge records (Caine, unpublished data) with the 284 daily snowmelt estimates to obtain a daily yield from calculated snowmelt; since in a watertight basin with a short travel distance, continuity requires that daily discharge recorded at the weir equals or exceeds the daily volume of meltwater produced by the snowpack. It follows that an observation of the negative case may mean that the basin is not watertight. The process of comparing predicted snowmelt to measured discharge is summarized in Equation 5:

$$Q \geq a * \rho * A \qquad \text{[Eqn. 5]}$$

where Q is measured daily discharge in m^3d^{-1}, a is ablation in md^{-1}, ρ is snow density, and A is snowpack area in m^2. When this inequality fails to be true and predicted snowmelt exceeds measured discharge, I can say that the basin is losing water.

I compared the estimated snowmelt volume with gage records from Martinelli basin over the period 1991-2012, and found that Martinelli had an average daily yield equivalent to 39.4% of calculated snowmelt volume, with a standard deviation of 34.6% ($n = 284$). The inequality (Eqn. 5) returned false on all but eleven of the 284 days when a snowpack area measurement was taken, showing that water was lost consistently during these years. The curve fit suggests that the basin loses at least 500 m^3 d^{-1} during the post-peak melt season, which increases to ~600 m^3 d^{-1} (or 288 mm of specific underflow over the course of the melt season) with the addition of daily precipitation on measurement days (Fig. 46).
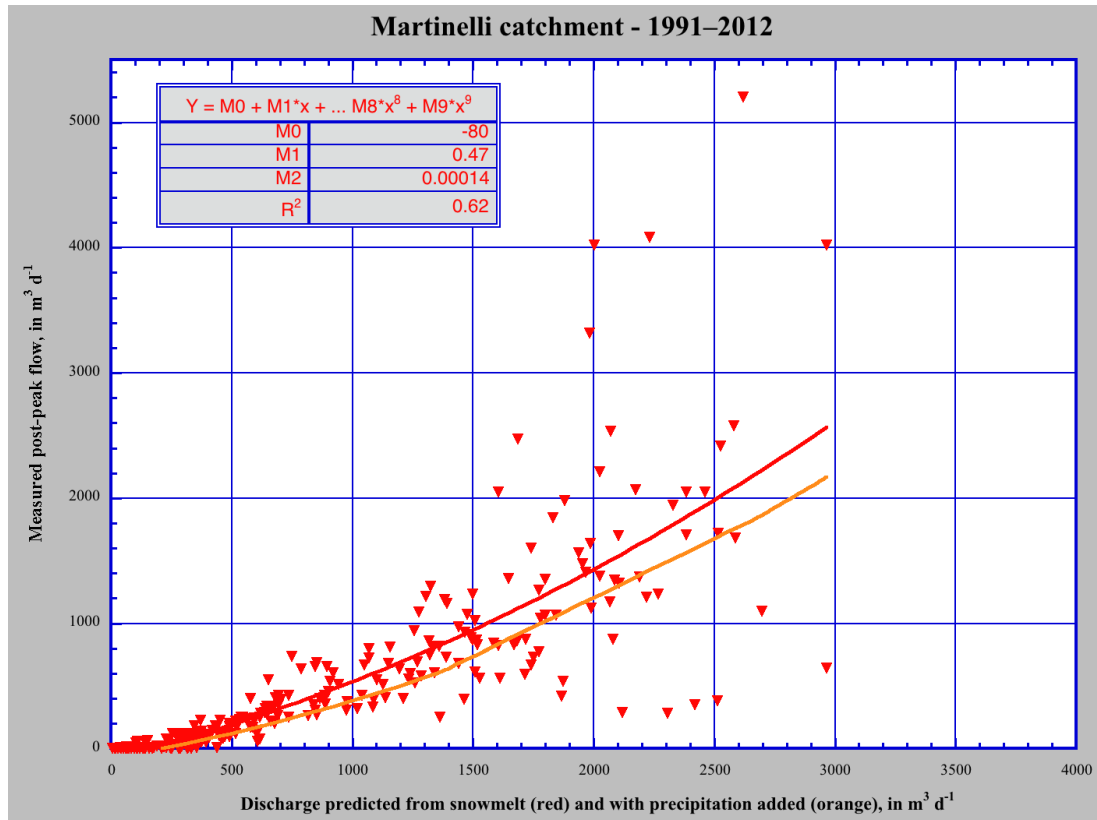
Figure 46. Discharge predicted from snowmelt versus measured post-peak flow in Martinelli. Trend with daily precipitation added to discharge prediction is shown in orange. Snowmelt-only trend shows a ~500 m³ d⁻¹ disparity between the predicted and measured values, snowmelt and precipitation trend shows a ~600 m³ d⁻¹ disparity. Outliers above the curve occur on days after significant rainfall events.

Calibration of underflow volume model

The same underflow volume model was applied to Martinelli in order to support findings from Saddle basin. Since I know the volume of underflow in Martinelli that occurs over the course of a year due to snowmelt, I can calibrate the underflow volume model by cross-checking its output with the underflow values calculated for Martinelli.

Table 8: Inputs and outputs of the subsurface carrying capacity model in Martinelli stream

Variable	Value	Unit
P_{tot}	218	mm

Q_{tot}	45	mm
A_{basin}	250	ha
T	50	days
U_{avg}	865	$m^3 \ d^{-1}$

The model shows that approximately 865 $m^3 \ d^{-1}$ of water underflow the Martinelli

gage during the period *T*, or approximately 10 L s^{-1} on average. Over the period, this

equates to 173 mm of specific underflow. If I assume 40% E and ET influence as in

Saddle, the specific underflow is reduced to -20.2 mm, which again cannot be true. Thus

it is again likely that E and ET are overestimates. If I assume that the above underflow

values derived from predicted versus measured snowmelt are correct, E and ET estimates

for the basin must be reduced.

Geophysical study

Saddle basin geophysical measurements

Dr. Matthias Leopold of the Technical University of Munich collected electrical

resistivity tomography (ERT) data with Gabriel Lewis (Williams College) in a location

crucial to this study, approximately 25m above the source of the Saddle stream, at an

elevation just above 3500 m. The purpose of the study was to discover whether the cold

water temperatures measured at the spring source at the top of the stream (Fig. 33b;

location 014) were caused by melting of one or more local ice lenses. Lewis et al. (2012)

interpret ERT data as showing no ice lens, and relatively warm temperatures in the

subsurface, but they find silty, gravelly sand over openwork cobble gravel starting at ~70

cm depth and extending more than 5 meters into the subsurface (Fig. 47). The survey

indicated bedrock was buried more than 5 m deep in the subsurface. In order to

accommodate ~2°C temperatures as seen at Saddle location 014 throughout the melt

season, an annual temperature-depth model from Lewis et al. (2012) indicates that

groundwater must have traveled at 2-3m depth to have acquired that ambient

temperature.
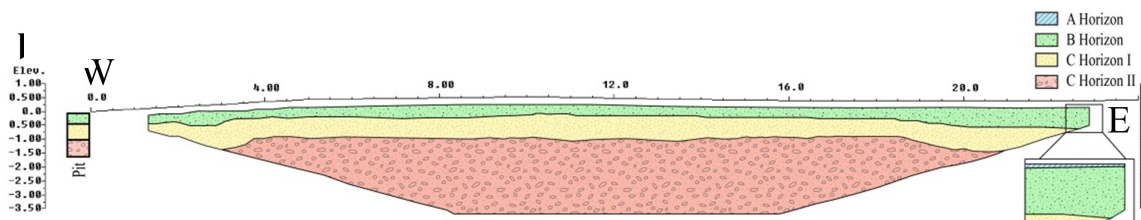
Figure 47: Profile derived from ERT data above Saddle stream source, showing stratigraphic interpretation based on measured resistivity and two ground-truth pits dug to 1.0 and 1.5 m depth. C horizons I and II indicate layers with higher measured resistivity values, which in this case are an indication of increased permeability. Inset: closeup showing the top layers of the section (from Lewis et al., 2012).

Martinelli basin geophysical measurements

A shallow subsurface seismic refraction study (Leopold et al., 2008) was

conducted just above the three well locations at ~3430 m in Martinelli (Fig. 10) as a

cross-section through the basin's lowest wetland. The study found evidence of a fine-

grained stratigraphic layer overlying coarse periglacial sediment beneath the flanks of the

basin, and bedrock in the center (Fig. 48). Bedrock could be fractured (and thus

hydrologically permeable), but without a conclusive ground-truth study, this remains

unknown.
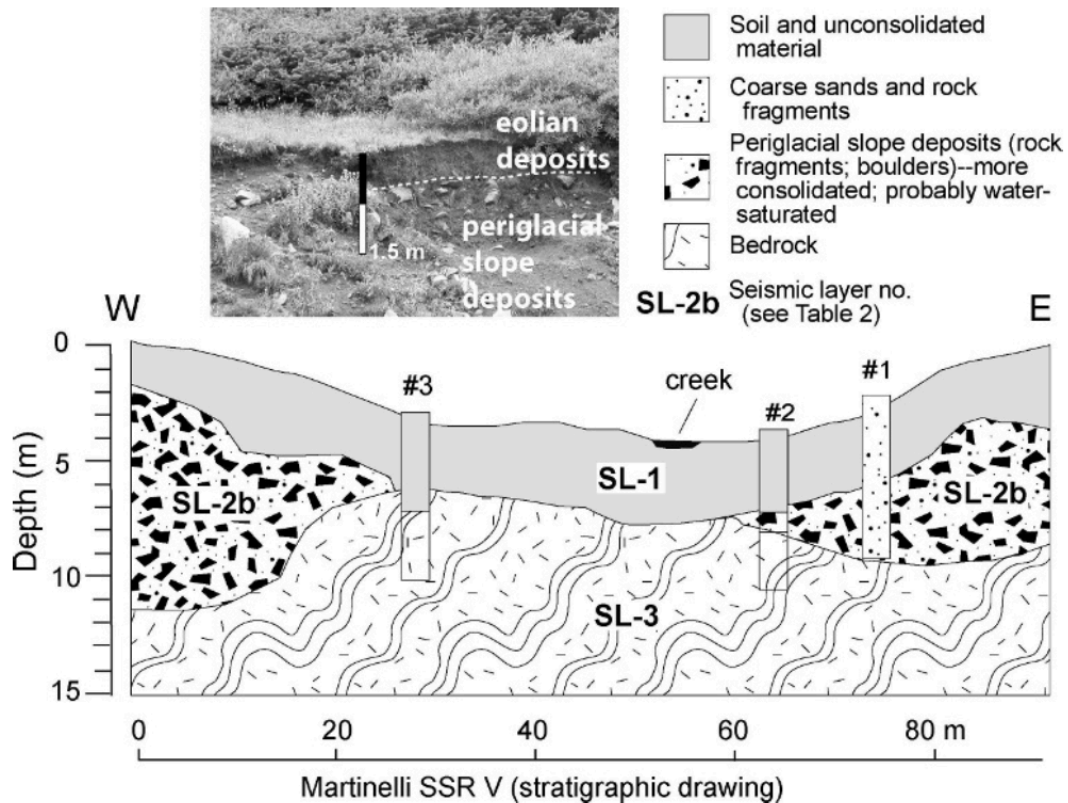
Figure 48. Cross-basin subsurface composition in Martinelli basin (from Leopold et al., 2008). Interpreted borehole data for three wells used in groundwater study are labeled. Inlay: ground truth cross-section from the right side of Martinelli basin showing coarse periglacial slope deposits overlain by ~0.5 m of fine, eolian-rich deposits.

The big picture

Since it is difficult to directly measure the underflow of unglaciated basins, it is imperative that water budget studies find ways to estimate and measure it indirectly. In Saddle stream, the results show a consistent loss of discharge over distance. Short-term hydrologic yield calculations indicate significant underflow. Although the discharge in Saddle stream is much more difficult to predict than in its counterpart, the size of the hydrologic conduits that exist beneath the stream can be estimated using the July 5–10 rain event.

84

Calculations made of predicted snowmelt in the Martinelli basin clearly show that underflow is carrying approximately 30% of the basin's discharge past the weir. Although Martinelli streamflow change down-channel is not as conspicuous as that in Saddle stream, Martinelli yields almost as little surface water at its gage. Evidence of this is visible in the wetland skirt just below the snowfield, where snowmelt runs for less than 20m, then disappears entirely into the hillslope deposits at low and medium flow (Figs. 17, 18) and does not reappear for at least another 100 m downslope.

Discharge, temperature, and groundwater depth results from the Martinelli basin suggest groundwater elevation is related to surface water discharge in the basin. Predicted daily values of snowmelt for the basin exceed measured daily yield, especially at low flow. This alone suggests water is eluding the gage. However, because snowmelt is not the only input to summer discharge in Martinelli (a steep basin without significant vegetation where ET and E are probably low), it is significant that the daily yield volume only exceeds the daily snowmelt volume estimate on 11 days when $n = 284$ implies strongly that some process or alternate hydrologic pathway is allowing discharge to elude the gage.

According to analysis of discharge versus snowpack area over 21 years in Martinelli basin, groundwater-accommodating conduits in the basin subsurface transmit approximately 600 m^3 d^{-1}. Due to Darcy's law (Darcy, 1856), groundwater transmission volume during and immediately after significant precipitation events may be much greater due to increased head values and area.

The complete picture is much more complex and detailed than I can currently model. However, a simple model made from carefully observed ground truth helps

illustrate the hydrogeological processes at work in the basin. Fig. 49 is a schematic

interpretation of water table depth and shows its interaction with the surface at high and

low flows in Martinelli basin.
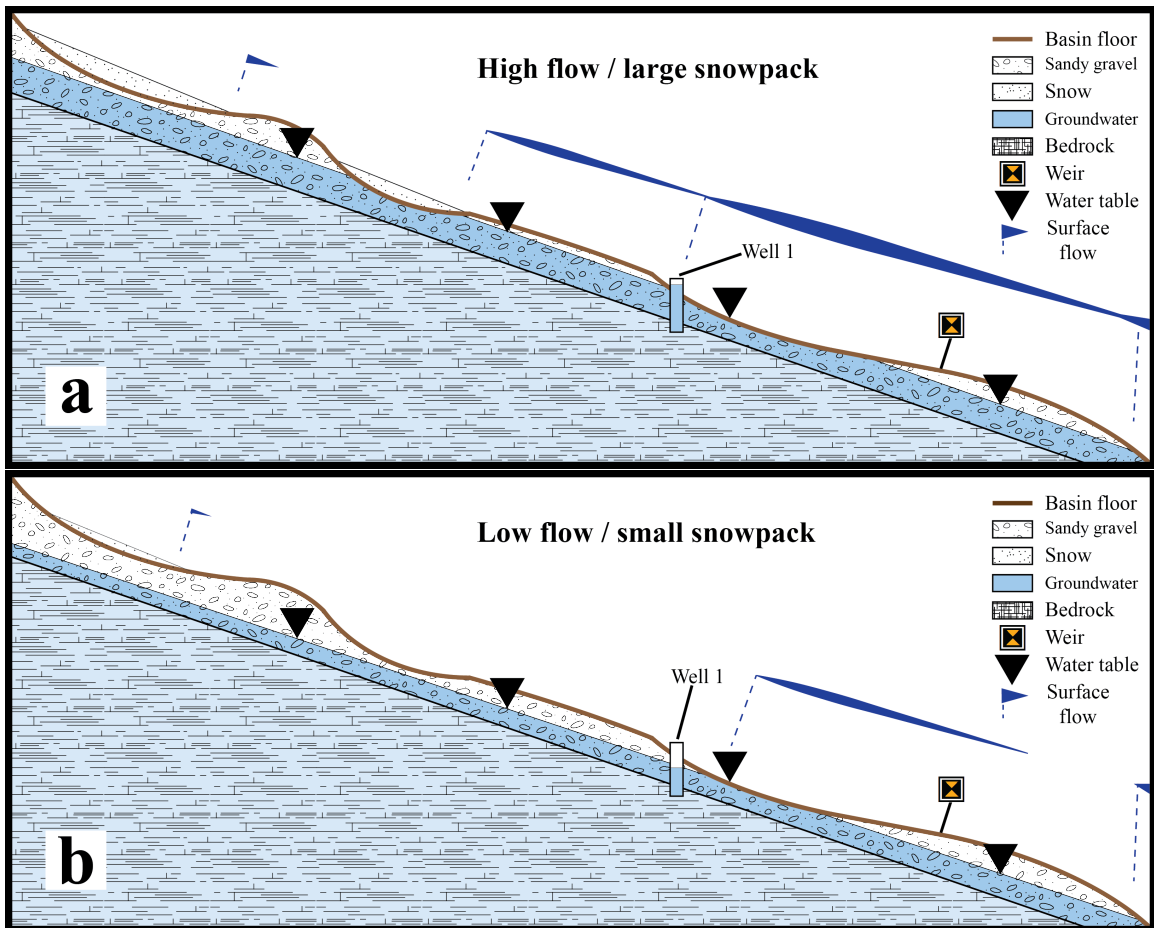
Figure 49. Downsection sketch showing groundwater depth in Martinelli basin at a. high flow and b. low flow. Surface flow indicator flags denote approximate relative discharge. Flagpoles indicate locations of significant additions to surface flow. Groundwater may also flow in and out of the pane of the sketch due to groundwater inflow and outflow across basin limts. Locations where groundwater and the ground surface intersect indicate hyporheic zones or wetland areas. Note that surface flow decreases when the water table lies significantly below the ground surface. Water depth in well is a schematic representation of head. During spring high flows, pressures in the well are artesian (water level in the well rises above the ground surface). Topography is approximate and vertically exaggerated to highlight water table interaction with the ground surface.

ERT data (and soil pits) suggest that stratigraphic layers on the south-facing slope of Niwot Ridge can accommodate large volumes of water. Due to the fact that this surface is covered in inactive periglacial features, it is reasonable to hypothesize that Quaternary periglacial processes buried gravel layers such as that described by Lewis (2012) or previous channels where Martinelli and Saddle basins exist at present. Due to conclusions drawn in Leopold et al. (2008), eolian sediment transport likely helped to bury these layers.

Borehole data for Saddle indicate that "little aquifers" exist at varying (or multiple) depths in the stratigraphy on the top of the Saddle ridge (King, 2012, p. 41), some of which had artesian pressures, at depths 10 m. Downstream, discharge of 0.6 L s^{-1} disappeared between Saddle locations 010 and 009 at low flow this field season, which equates to roughly 50 m^3 d^{-1}. More significantly, a model of subsurface carrying capacity suggests that between 25 mm and 173 mm of specific underflow occurs in the Saddle basin per year.

In Martinelli basin, the minimum underflow and escape value discussed above equates to 288 mm per year. In other words, more than a quarter of total precipitation goes unrecorded due to underflow.

Heath (1982) states that just a 1-m^2 cross-section of gravel bed can transmit 100 m^3 to approximately 5000 m^3 of groundwater flow per day, so only a small cross section of a sand or gravel lens is needed to accommodate the missing discharge in the basins. Since the depth to bedrock equals or exceeds 5 m in many places in both Martinelli and Saddle basins, one or several cross-sectional lenses composed of sand or coarser material

could account for significant underflow. Thus, losses to groundwater are likely capable of accounting for bypass in the basins.

Water budgets

My work shows that underflow accounts for some of the missing flow in Saddle basin (Fig. 50). However, over-reported values of E and ET, and possibly underreported values of P cause a water budget overestimate. Since Saddle's weir is below treeline, ET is likely an important process, but the value reported by Greenland (1989) is likely an overestimate (Laghari et al., 2012). I have shown that E values reported in Hood et al. (2010), Knowles et al. (2012), and Greenland (1989) are likewise overestimates for the basins. However because my work relies on these values, I am forced to use them.

Underflow estimates for Martinelli basin are better constrained than those for Saddle. Using the average annual underflow value determined from differences in discharge and predicted snowmelt from N. Caine's (unpublished data) measurements (288 mm), I estimate the water budgets of both basins (Fig. 51) and the data implicate that certain reported hydroclimatic values could be incorrect for these basins.
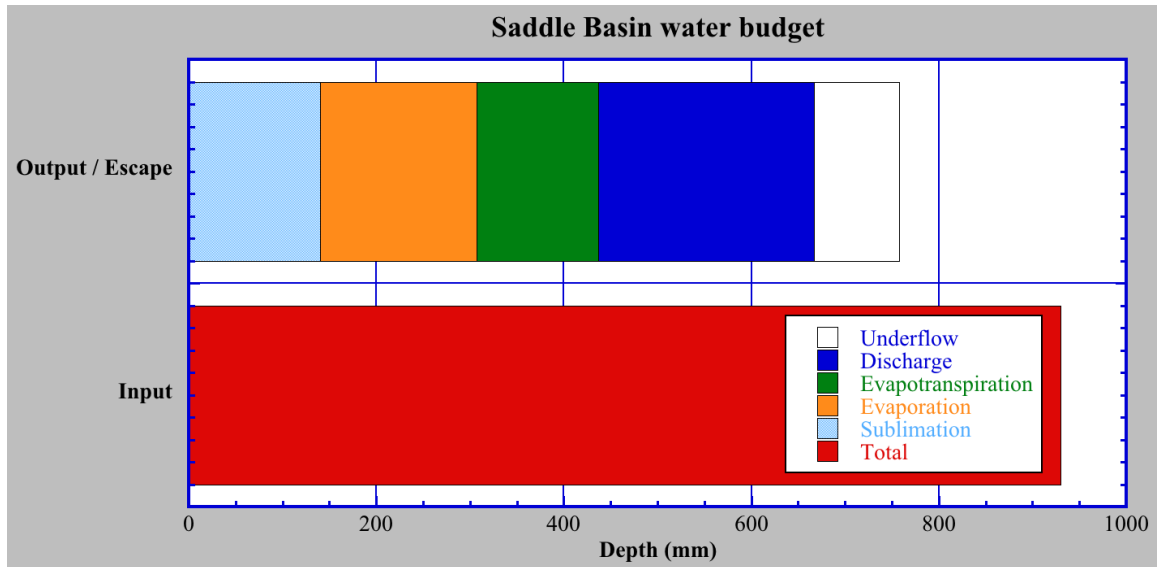
Figure 50. Saddle basin water budget. Precipitation: 930 mm (NRCS, 2012); underflow: 91 mm; runoff: 230 mm (NWLTER, 2012); ET: 260 mm (Greenland, 1989); E: 223 mm (Knowles et al., 2012); sublimation: 140 mm (Hood et al., 2010).
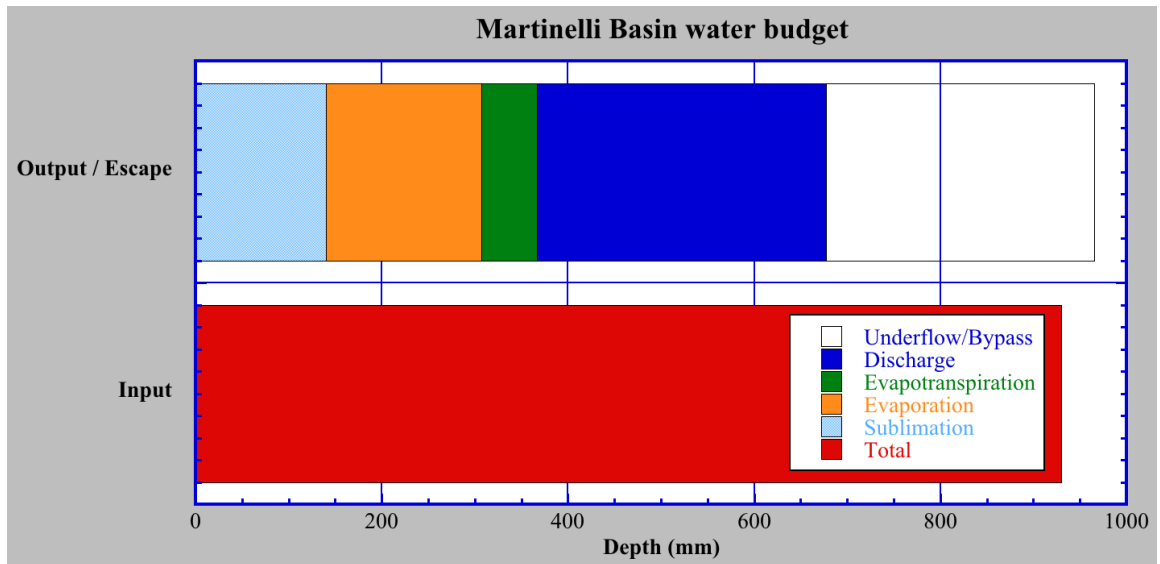
Figure 51. Martinelli basin water budget. Precipitation: 930 mm (NRCS, 2012); underflow: 288 mm; runoff: 310 mm (Caine, unpublished); ET: 260 mm (modified from Greenland, 1989); E: 223 mm (modified from Knowles et al., 2012); sublimation: 140 mm (Hood et al., 2010).

Both water budgets show a discrepancy between input and output values in these basins. Since the snowpack is built up with windblown snow from outside the basin, it is

possible that P is higher than reported, and that E and ET are lower than reported. Snow

redistribution has been cited (Bernhardt et al., 2012; DeBeer et al., 2010 Dery et al.,

2001; Erickson et al., 2005) for increased precipitation input, which could account for

part of the discrepancy. Since three unglaciated basins (Martinelli, Saddle, and Como) lie

in a row, it is possible that snow redistribution due to strong west winds during the winter

results in greater than reported P values for these basins.

CONCLUSIONS

The study shows that some flow bypasses the gages at Martinelli and Saddle streams, contributing to the disparity between inputs and outputs for basin water budgets and similar to that reported for Como Creek. Bypass is likely due to permeable, subsurface stratigraphic layers that provide hydrologic pathways to downgradient areas.

Modeling indicates that the weir at Martinelli records at most 75% of the flow it receives from snowmelt and precipitation. This equates to a bypass of approximately 600 $m^3 d^{-1}$ on a typical post-peak day in the melt season, or 288 mm (30% of total annual input).

At low flow, Saddle stream loses 50 cubic meters per day (20 mm or 2% of total annual input) from the channel between locations 010 and 009. More complex calculations suggest that at least 10% (91 mm, or 232 $m^3 d^{-1}$) of total Saddle basin input is lost to underflow.

In other unglaciated alpine basins, discharge should be used as a proxy for precipitation only where other components of the water budget can be carefully evaluated. It is also useful to include underflow values in the water budgets of basins like this.

Future work

Future work should include recording more comprehensive measurements with greater resolution over the areas of interest in the two basins. Greater data density will likely yield more conclusive results, especially in the case of Saddle, where the

snowpack–discharge relationship is not well known because snowpack measurements are not available in the quantity that exists in Martinelli basin.

Another rewarding research route might be to attempt to find the emergence points of flow in these basins downslope and outside of this field season's study boundaries, using the same techniques described in this study. Accessibility and minimal field time were limiting factors to downslope exploration, but it is likely that finding an outlet for water would give clues as to the types of processes taking place in the basin.

Tracer studies in these basins would shed light on hydrologic transmission times and the geographic locations of flow pathways and emergence points in the basin, both of which are still poorly understood, especially in Saddle basin, where no tracer study has ever been done before. However, given the tight regulations placed on the watershed by the City of Boulder, it may be challenging to obtain the permission to do a study like this.

REFERENCES

Anderson, R.S., and Anderson, S.P., 2010, Geomorphology: The Mechanics and Chemistry of Landscapes: Cambridge University Press, Cambridge, UK.

Anderson, S.P., and Von Blackenburg, F., 2007, Mechanical-chemical interactions shape the Critical Zone and fluxes from it: Elements, October.

Anderson, S.P., Qinghua, G., and Parrish, E.G., 2012, Snow-on and snow-off LiDAR point cloud data and digital elevation models for study of topography, snow, ecosystems and environmental change at Boulder Creek Critical Zone Observatory, Colorado, Boulder Creek CZO, INSTAAR, University of Colorado at Boulder.

Benedict, J.B., 1970, Downslope soil movement in a colorado alpine region: rates, processes, and climatic significance: Arctic and Alpine Research, v. 2, no. 3, p. 165–226.

Berg, N.H., 1986, Blowing snow at a Colorado alpine site: measurements and implications: Arctic and Alpine Research, v. 18, no. 6, p. 147–161.

Bernhardt, M., Schulz, K., Liston, G.E., and Zängl, G., 2012, The influence of lateral snow redistribution processes on snow melt and sublimation in alpine regions: Journal of Hydrology, v. 424-425, p. 196–206, doi: 10.1016/j.jhydrol.2012.01.001.

Bierman, P., and Montgomery, D., 2013, Geomorphology: W.H. Freeman & Company, New York, NY.

Bowman, W.D., and Seasteadt, T.R. (Eds.), 2001, Structure and Function of an Alpine Ecosystem; Niwot Ridge, Colorado: Oxford University Press, Oxford, UK.

Caine, N., 1989a, Diurnal variations in the inorganic solute content of water draining from an alpine snowpatch: Catena, v. 16, no. 2, p. 153–162, doi: 10.1016/0341-8162(89)90038-6.

Caine, N., 1989b, Hydrograph separation in a small alpine basin based on inorganic solute concentrations: Journal of Hydrology, v. 112, no. 1-2, p. 89–101, doi: 10.1016/0022-1694(89)90182-0.

Caine, N., 1992a, Modulation of the diurnal streamflow response by the seasonal snowcover of an alpine basin: Journal of Hydrology, v. 137, no. 1-4, p. 245–260, doi: 10.1016/0022-1694(92)90059-5.

Caine, N., 1992b, Sediment Transfer on the Floor of the Martinelli Snowpatch, Colorado Front Range, U. S. A.: Geografiska Annaler. Series A, Physical Geography, v. 74, no. 2/3, p. 133–144, doi: 10.2307/521291.

Caine, N., 1995a, Snowpack Influences on Geomorphic Processes in Green Lakes Valley, Colorado Front Range: The Geographical Journal, v. 161, no. 1, p. 55, doi: 10.2307/3059928.

Caine, N., 1995b, Temporal Trends in the Quality of Streamwater in an Alpine Environment: Green Lakes Valley, Colorado Front Range, U. S. A.: Geografiska Annaler. Series A, Physical Geography, v. 77, no. 4, p. 207, doi: 10.2307/521330.

Caine, N., and Swanson, F., 1989, Geomorphic coupling of hillslope and channel systems in two small mountain basins: Zeitschrift fuer Geomorphologie, p. 189–203.

Clow, D.W., Schrott, L., Webb, R., Campbell, D.H., Torizzo, A., and Dornblaser, M., 2003, Ground Water Occurrence and Contributions to Streamflow in an Alpine Catchment, Colorado Front Range: Groundwater, v. 41, no. 7, p. 937–950.

Cole, J.C., and Braddock, W.A., 2009, Geologic map of the Estes Park 30' x 60' quadrangle, north-central Colorado: U.S. Geological Survey Scientific Investigations Map 3039, 1 sheet, scale 1:100,000, pamphlet, 56 p.

Cowie, R., 2011, The hydrology of headwater catchments from the plains to the continental divide, Boulder Creek Watershed, Colorado [Masters thesis]: University of Colorado at Boulder.

Darcy, H., 1856, Les Fontaines Publiques de Ville de Dijon, Dalmont, Paris.

Day, C.A., 2009, Modelling impacts of climate change on snowmelt runoff generation and streamflow across western US mountain basins: a review of techniques and applications for water resource management: Progress in Physical Geography, v. 33, no. 5, p. 614–633, doi: 10.1177/0309133309343131.

DeBeer, C.M., and Pomeroy, J.W., 2010, Simulation of the snowmelt runoff contributing area in a small alpine basin: Hydrology and Earth System Sciences, v. 14, no. 7, p. 1205–1219, doi: 10.5194/hess-14-1205-2010.

Déry, S., and Yau, M., 2001, Simulation of blowing snow in the Canadian Arctic using a double-moment model: Boundary-Layer Meteorology, no. 1997, p. 297–316.

Erickson, T. a., Williams, M.W., and Winstral, A., 2005, Persistence of topographic controls on the spatial distribution of snow in rugged mountain terrain, Colorado, United States: Water Resources Research, v. 41, no. 4, p. n/a–n/a, doi: 10.1029/2003WR002973.

Gable, D.J., 2000, Geologic map of the Proterozoic rocks of the central Front Ranges, Colorado: U.S. Geological Survey, Denver, CO.

Gable, D.J., and Madole, R.F., 1976, Geologic map of the Ward quadrangle, Boulder County, Colorado: U.S. Geological Survey, Denver, CO.

Greenland, D., 1989, The Climate of Niwot Ridge, Front Range, USA: Arctic and Alpine Research, v. 21, no. 4, p. 380–391.

Gutmann, E.D., Larson, K.M., Williams, M.W., Nievinski, F.G., and Zavorotny, V., 2012, Snow measurement by GPS interferometric reflectometry: an evaluation at Niwot Ridge, Colorado: Hydrological Processes, v. 26, no. 19, p. 2951–2961, doi: 10.1002/hyp.8329.

Hamann, H.B., 1998, Snowcover Controls on Alpine Soil Surface Temperature Patterns: [Masters thesis] University of Colorado at Boulder.

Heath, R.C., 1987, Basic Ground-Water Hydrology. United States Geological Survey Paper 2220: U.S. Geological Survey, Reston, VA. 84 p.

Heath, R.C., 1982, Classification of Ground-Water Systems of the United States: Ground Water, v. 20, no. 4, p. 393–401, doi: 10.1111/j.1745-6584.1982.tb02758.x.

Herzfeld, U.C., Mayer, H., Caine, N., Losleben, M., and Erbrecht, T., 2003, Morphogenesis of typical winter and summer snow surface patterns in a continental alpine environment: Hydrological Processes, v. 17, no. 3, p. 619–649, doi: 10.1002/hyp.1158.

Hood, E., Williams, M., and Cline, D., 1999, Sublimation from a seasonal snowpack at a continental, mid-latitude alpine site: Hydrological Processes, v. 13, no. 12-13, p. 1781–1797, doi: 10.1002/(SICI)1099-1085(199909)13:12/13<1781::AID-HYP860>3.0.CO;2-C.

Jepsen, S.M., Molotch, N.P., Williams, M.W., Rittger, K.E., and Sickman, J.O., 2012, Interannual variability of snowmelt in the Sierra Nevada and Rocky Mountains, United States: Examples from two alpine watersheds: Water Resources Research, v. 48, no. 2, doi: 10.1029/2011WR011006.

Kantack, K.M., 2011, Reconstructing Pinedale (latest Pleistocene) ice in the Green Lakes Valley and adjacent areas, Colorado [Undergraduate thesis]: Williams College.

Kellogg, D.Q., Gold, A.J., Groffman, P.M., Stolt, M.H., and Addy, K., 2008, Riparian Ground-Water Flow Patterns Using Flownet Analysis: Evapotranspiration-Induced Upwelling and Implications for N Removal: JAWRA Journal of the American Water Resources Association, v. 44, no. 4, p. 1024–1034, doi: 10.1111/j.1752-1688.2008.00218.x.

King, J.J., 2012, Characterization of the shallow hydrogeology with estimates of recharge at a high-altitude mountainous site, Niwot ridge, Front Range, Colorado [Masters thesis]: University of Colorado at Boulder.

Knowles, J.F., Blanken, P.D., Williams, M.W., and Chowanski, K.M., 2012, Energy and surface moisture seasonally limit evaporation and sublimation from snow-free alpine tundra: Agricultural and Forest Meteorology, v. 157, p. 106–115, doi: 10.1016/j.agrformet.2012.01.017.

Kuchment, L.S., and Gelfan, A.N., 1996, The determination of the snowmelt rate and the meltwater outflow from a snowpack for modelling river runoff generation: Journal of Hydrology, v. 179, no. 1-4, p. 23–36, doi: 10.1016/0022-1694(95)02878-1.

Laghari, A.N., Vanham, D., and Rauch, W., 2012, To what extent does climate change result in a shift in Alpine hydrology? A case study in the Austrian Alps: Hydrological Sciences Journal, v. 57, no. 1, p. 103–117.

Lapp, S., Byrne, J., Townshend, I., and Kienzle, S., 2005, Climate warming impacts on snowpack accumulation in an alpine watershed: International Journal of Climatology, v. 25, no. 4, p. 521–536, doi: 10.1002/joc.1140.

Leopold, M., Dethier, D.P., Raab, T., Rikert, T.C., and Caine, N., 2008, Using Geophysical Methods to Study the Shallow Subsurface of a Sensitive Alpine Environment, Niwot Ridge, Colorado Front Range, U.S.A.: v. 40, no. 3, p. 519–530, doi: 10.1657/1523-0430(06-124).

Leopold, M., Völkel, J., Dethier, D., Williams, M.W., and Caine, N., 2010, Mountain Permafrost – A Valid Archive to Study Climate Change? Examples from the Rocky Mountains Front Range of Colorado, USA: Nova Acta Leopoldina, v. 289, no. 384, p. 281–289.

Lewis, G.M., Leopold, M., and Dethier, D.P., 2012, Using Geophysical Techniques in the Critical Zone to Determine the Presence of Permafrost: Geological Society of America Abstracts with Programs, v. 44-7, p. 460.

Liu, F., Williams, M.W., and Caine, N., 2004, Source waters and flow paths in an alpine catchment, Colorado Front Range, United States: Water Resources Research, v. 40, no. 9, doi: 10.1029/2004WR003076.

Lovering, T., and Goddard, E., 1950, Geology and Ore Deposits of the Front Range, Colorado: U.S. Geological Survey, Washington, D. C.

Madole, R.F., 1982, Possible Origins of Till-like Deposits Near the Summit of the Front Range in North-Central Colorado: Geological Survey Professional Papers, no. 1243. 31 p.

Martinelli, M., 1959, Some hydrologic aspects of Alpine snowfields under summer conditions: Journal of Geophysical Research, v. 64, no. 4, p. 451, doi: 10.1029/JZ064i004p00451.

McClymont, A.F., Roy, J.W., Hayashi, M., Bentley, L.R., Maurer, H., and Langston, G., 2011, Investigating groundwater flow paths within proglacial moraine using multiple geophysical methods: Journal of Hydrology, v. 399, no. 1-2, p. 57–69, doi: 10.1016/j.jhydrol.2010.12.036.

Miller, W.P., and Piechota, T.C., 2011, Trends in Western U.S. Snowpack and Related Upper Colorado River Basin Streamflow: JAWRA Journal of the American Water Resources Association, v. 47, no. 6, p. 1197–1210, doi: 10.1111/j.1752-1688.2011.00565.x.

Molotch, N.P., Blanken, P.D., Williams, M.W., Turnipseed, A.A., Monson, R.K., and Margulis, S.A., 2007, Estimating sublimation of intercepted and sub-canopy snow using eddy covariance systems: Hydrological Processes, v. 21, no. 12, p. 1567–1575, doi: 10.1002/hyp.6719.

Molotch, N.P., Meixner, T., and Williams, M.W., 2008, Estimating stream chemistry during the snowmelt pulse using a spatially distributed, coupled snowmelt and hydrochemical modeling approach: Water Resources Research, v. 44, no. 11, p. 1–14, doi: 10.1029/2007WR006587.

Muir, D.L., Hayashi, M., and McClymont, A.F., 2011, Hydrological storage and transmission characteristics of an alpine talus: Hydrological Processes, v. 2966, no. March, p. 2954–2966, doi: 10.1002/hyp.8060.

National Resource Conservation Service, 2013, University Camp (838) - Site Information and Reports: National Water and Climate Center, United States Department of Agriculture.

Niwot Ridge Meteorology/Climatology, 2012, Niwot Ridge Long-Term Ecological Research program: Niwot Ridge Long-Term Ecological Research program.

Parman, J.N., 2010, Climatological and elevational controls on organic and inorganic nutrients in stream waters, Boulder Creek Watershed, Colorado Front Range [Masters thesis]: University of Colorado Boulder.

Rantz, S., 1964, Snowmelt Hydrology of a Sierra Nevada Stream: Contributions to the Hydrology of the United States: Geological Survey water supply paper, v. 1779-R.

Scanlon, B., Healy, R., and Cook, P., 2002, Choosing appropriate techniques for quantifying groundwater recharge: Hydrogeology Journal, v. 10, no. 1, p. 18–39, doi: 10.1007/s10040-001-0176-2.

Strahler, A.N., 1957, Quantitative Classification of Watershed Geomorphology: Transactions, American Geophysical Union, v. 38, no. 6, p. 915–920. <http://www.prism.washington.edu/file/show/1767>

Strasser, U., Bernhardt, M., Weber, M., Liston, G.E., and Mauser, W., 2008, Is snow sublimation important in the alpine water balance?: The Cryosphere, v. 2, no. 1, p. 53–66.

Sueker, J.K., Ryan, J.N., Kendall, C., and Jarrett, R.D., 2000, Determination of hydrologic pathways during snowmelt for alpine/subalpine basins, Rocky Mountain National Park, Colorado: Water Resources Research, v. 36, no. 1, p. 63–75.

United States Army Corps of Engineers, 1998, Engineering and Design--Runoff from Snowmelt: Engineering Manual 1110-2-1406.

United States Geolgical Survey, 1999, Digital Orthophoto Quarter-Quadrangles, Menlo Park, CA.

Williams, M.W., Barnes, R.T., Parman, J.N., Freppaz, M., and Hood, E., 2011, Stream Water Chemistry along an Elevational Gradient from the Continental Divide to the Foothills of the Rocky Mountains: Vadose Zone Journal, v. 10, no. 3, p. 900, doi: 10.2136/vzj2010.0131.

Wilson, J., and Guan, H., 2004, Mountain-block hydrology and mountain-front recharge, *in* Hogan, J.F., Phillips, F.M., and Scanlon, B.R. eds., Groundwater Recharge in a Desert Environment: The Southwestern United States, Volume 9, American Geophysical Union, Washington, D. C., p. 113–137.

Winkler, J.N., 2012, The hydrology and geochemistry of two snowmelt-dominated, alpine streams in the Boulder Creek Critical Zone Observatory, Front Range, Colorado [Undergraduate thesis]: The University of Connecticut.